

Chapter 6: Results and Initial Conclusions

6.1 Results of Osteometric Analysis

As few known castrate skeletons are intact and readily available, it was only possible to study the skeletons of two individuals. The first was a castrate whose skeleton is at the Medical University Anatomical Museum, Lyon, France. The second was Nekht-Ankh, one of the Two Brothers mummies in the University Museum, Manchester, England. These two individuals will be compared to the Tandler and Grosz skeleton, the two Ming Dynasty skeletons, and the available information for Farinelli discussed in Chapter 5. The full skeletal reports for the Lyon castrate and Nekht-Ankh are presented in Appendix 1.

6.1.1 Humans

6.1.1.1 Morphological Analysis

6.1.1.1.1 Lyon Skeleton

The major visible changes in the skeleton are the exaggerated length of the long bones due to the delay of epiphyseal fusion and the developmental changes in the ossa coxae and craniofacial area caused by the lack of sex hormones. These changes were expected, as they have been part of the description of castrates for centuries (as outlined in the previous chapter). This study has found additional changes to the skeletons of prepubertal castrates that were either not known or not clearly defined.

According to Lortet,⁴⁷⁵ the Lyon castrate is of African origin, from the Shillouk people of modern-day Sudan. The skeleton is wired and glued into anatomical articulation and hangs upright in a case in the museum. When viewing the skeleton in a vertical position, it is possible to see a

⁴⁷⁵ (1896)



Figure 6.1: The Lyon castrate hanging in the museum case, showing the disproportion visible in the skeleton. Photograph by author.

disproportion in the skeleton similar to the proportional nonconformities in living castrates observed by Pittard and Wagenseil.⁴⁷⁶ The hands hang by the knees, and the lower limbs are much longer than the torso. The pelvis appears small and oddly shaped, and the large, robust mandible dominates the face (**Figure 6.1**). However, once the skeleton is laid out horizontally for examination, most of the visual skeletal disproportion disappears, except in the hands and feet.

When Lortet discussed the twenty millimetre difference in measured and calculated stature for the Lyon castrate, he may have been highlighting a problem with stature regression methods. The current popular stature regression method, created by Trotter and Gleser, relies on linear regression to create stature formulae, as did Rollet's method.⁴⁷⁷ These formulae are highly population specific, and can lead to the overestimation of stature in short individuals and the underestimation of stature in tall individuals.⁴⁷⁸ Therefore, the excess length of the long bones caused by the delayed epiphyseal fusion, in addition to causing disproportion, may have caused the stature of the skeleton to be severely underestimated by Rollet's method.



Figure 6.2: Detailed anterior and left lateral views of the skull of the Lyon castrate. Photo by author.

The mandible is heavy and square, with little build-up of the mental eminence, a broad, short ramus, and a shallow mandibular notch (**Figure 6.2**). The maxilla is strongly prognathic, with a very obvious fusion line between the two maxillary bones, and the

⁴⁷⁶ (Pittard, 1934; Wagenseil, 1933a, 1927)

⁴⁷⁷ (Jantz, 1992; Rollet, 1889; Trotter and Gleser, 1958)

⁴⁷⁸ (Duyar and Pelin, 2003; Sjøvold, 1990)

zygomas and zygomatic arches are delicate and do not extend past the external auditory meatus. The mastoid processes are short and anteriorly angled. There is no development of the superciliary ridges, the supraorbital margins are somewhat sharp, the orbits are trapezoidal in shape, and there is no evidence of the nuchal crest or the external occipital protuberances, giving the skull a very feminine appearance.

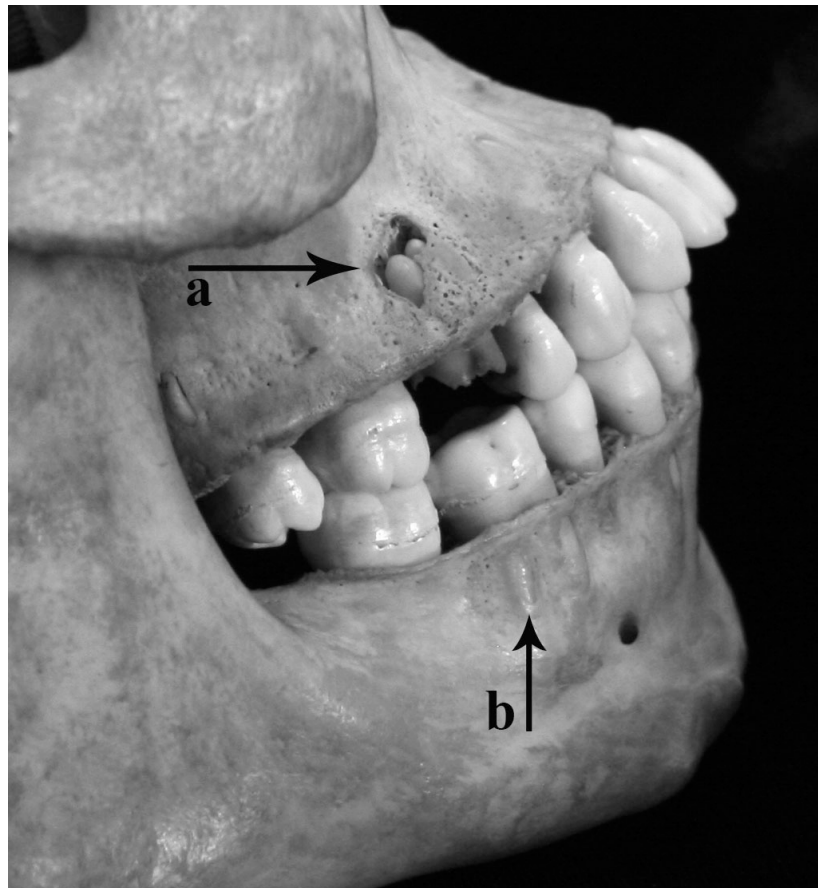


Figure 6.3: Dentition of the Lyon castrate, displaying the abscess caused by the incomplete removal of the right upper first molar (a) and the resorption of the alveolar bone (b). Photo by author.

The adult dentition is erupted, and the maxillary third molars are present, but the mandibular third molars are absent. As the alveolar bone is smooth and shows no signs of remodelling or indications that the third molars are about to erupt, this individual may not have possessed these teeth. There is slight calculus growth limited to the molars and lines of enamel hypoplasia are present on several teeth, most notably the upper second molars, approximately 1-2 mm from the dentine-enamel junction. It is possible that the enamel hypoplasia on the molars relates to the timing of the castration of the individual,

though it could also relate to childhood illness or malnutrition.⁴⁷⁹ The alveolar bone is very thin and has been resorbed along its superior and anterior surfaces, likely due to receding gums, exposing the roots of several teeth (**Figure 6.3**).

Both upper first molars have been sheared bilaterally at the dentine-enamel junction, possibly by a singular traumatic event, which resulted in the death of the roots, leaving them jagged and dead. On the right upper first molar, this appears to have resulted in an infection that created an abscess in the anterior surface of the maxilla. As there is little evidence of wear on the root surface, it is more likely that this damage was due to a singular traumatic event rather than slow, activity-related wear. There is some remodeling around the rim of the abscess, indicating that the abscess was only partially healed at time of death (**Figure 6.3**), which, coupled with the jagged edge of the roots, indicates that the teeth were damaged shortly before death, but not perimortem. The cause of the tooth removal is unclear, but as it is bilateral, it was likely either deliberate or a result of repeated activity, such as the duties he performed in the household for which he worked. It most likely is not linked to initiation rites having to do with his childhood kin group, as the roots are fully formed, which happens in modern populations around age ten, by which point he most likely was already castrated and employed in Cairo.

The long bones of the Lyon castrate are thin, long, and very gracile. This is most prominent in the hands and feet, which display the excess elongation of the extremities (**Figure 6.1**). All of the appendicular skeleton and most of the axial skeleton still possess open epiphyses. Few to no muscle attachment sites are visible, giving the impression of an individual who did not perform heavy labour. Most of the skeleton displayed evidence of osteoporosis, including high porosity on the vertebral bodies and thinning of the iliac fossae.

The Lyon castrate's true pelvis (the area of the pelvis containing the pelvic inlet and outlet and bounded by the ilium below the iliopectineal line, the pubis, the pubic rami, the ischium, the sacrum, and the coccyx) displays a mixture of masculine traits (small but upright, with a narrow, "V"-shaped subpubic angle and hooked sciatic notches) and feminine traits (wide and "D"-shaped obturator foramina, a thin ischiopubic ramus, and a shallow, less curved sacrum) (**Figure 6.4**). The ilia flare laterally and posteriorly at a very obtuse angle, forming a very wide but shallow false pelvis. The

⁴⁷⁹ (Ritzman et al., 2008)

acetabulae are very shallow and anterior and the pelvic outlet is narrow anterior-posteriorly, creating a triangular pelvic inlet. From the superior view of the pelvis, the ilia and true pelvis seem to form a “heart” shape. Epiphyses are either fusing or completely missing along the iliac crest and the ischium. The delay in fusion of the iliac crest could be causing the outward splay of the ilia.



Figure 6.4: Detailed anterior and superior views of the pelvis of the Lyon castrate, displaying the thinning of the iliac fossae and the shape of the subpubic angle and sciatic notches, with arrows marking the open epiphyses. Photo by author.

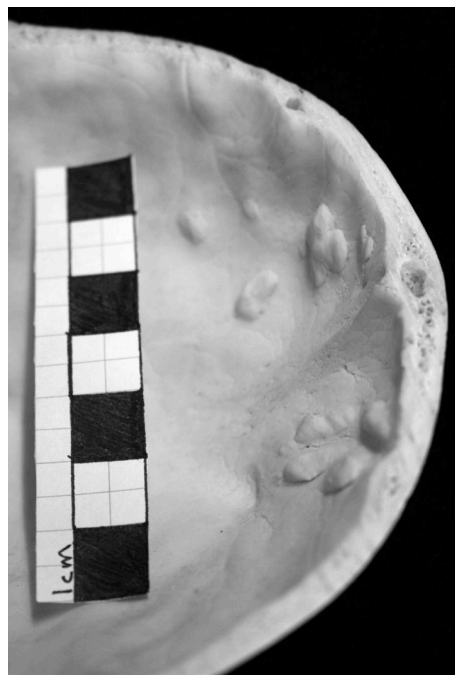


Figure 6.5: The internal table of the frontal bone of the Lyon castrate, showing early-stage *Hyperostosis Frontalis Interna*. Photo by author.

The Lyon castrate shows signs of *Hyperostosis Frontalis Interna* (HFI) on the internal table of his frontal bone (**Figure 6.5**). As he died in his early twenties, he would not have had long to develop the condition, but he appears to be between the first two of

Hershkovitz's four developmental stages of HFI.⁴⁸⁰ This stage is seen in modern women in their thirties.⁴⁸¹

Subsequent to the examination of the Lyon castrate, Belcastro and colleagues published work on the remains of Farinelli.⁴⁸² While Farinelli's remains were fragmentary, enough of a portion of his frontal bone had survived to suggest that he also had been affected by HFI.⁴⁸³ Farinelli possessed an advanced case of HFI, most likely due to a combination of his advanced age at death⁴⁸⁴ and his extended lack of exposure to androgenic steroids, which has been proven to encourage development of the condition (**Figure 6.6**).⁴⁸⁵ The presence of HFI in both the Lyon castrate and Farinelli suggests that this condition may be used as an indicator of castrate status.



Figure 6.6: Frontal bone from Farinelli, displaying the advanced state of *Hyperostosis Frontalis Interna* (from Belcastro et al., 2011).

6.1.1.1.2 Manchester Mummy

An examination of the Manchester mummy Nekht-Ankh was performed in order to assess the likelihood of his being a castrate. Nekht-Ankh's skeleton has been reassembled in anatomical position and mounted in a reclining position on a frame and backboard (**Figure 6.7**). This provided some logistical and methodological challenges in examining the skeleton that made it impossible to take certain measurements and to make certain age and sex assessments. It precluded the ability to photograph the superior

⁴⁸⁰ (Hershkovitz et al., 1999)

⁴⁸¹ (May et al., 2011)

⁴⁸² (Belcastro et al., 2011)

⁴⁸³ As discussed in Chapter Five.

⁴⁸⁴ (Belcastro et al., 2011)

⁴⁸⁵ (May et al., 2010)

view of the pelvic girdle. The interior of the skull could not be observed because of the size of the foramen magnum, which was too small to allow both a dental mirror and a light inside to inspect the interior. Thus it was not possible to assess whether HFI was present. Even with these restrictions, some discrepancies between the results of this examination of Nekht-Ankh and the original mummy report became apparent.⁴⁸⁶



Figure 6.7: Nekht-Ankh reassembled anatomically on a frame and wooden backboard. Photo by author; scale in cm.

Cameron, the attending physician, originally assessed Nekht-Ankh's age at sixty years by cranial suture closure. While this is a common ageing method, more accurate methods have been devised in the last hundred years.⁴⁸⁷ These include tooth eruption and wear (difficult in Egyptian populations given the generally gritty food consumed);⁴⁸⁸ epiphyseal fusion (already shown to be difficult in castrates);⁴⁸⁹ and developmental and degenerative changes in the fourth rib, the pubic symphysis, and the auricular surface (all of which were unavailable due to the articulation of the skeleton). All of Nekht-Ankh's teeth had erupted, including the third molars, indicating that he was older than twenty years, and all the teeth were highly worn, with the dentine exposed on most teeth but not

⁴⁸⁶ (Cameron, 1910)

⁴⁸⁷ (Brickley and McKinley, 2004; Buikstra and Ubelaker, 1994)

⁴⁸⁸ (Harris and Ponitz, 1980)

⁴⁸⁹ (Eng et al., 2010)

worn down to or past the roots, giving a minimum age of forty-five plus years by Brothwell's standard (**Figure 6.8**).⁴⁹⁰ As the ancient Egyptians are known to have additional wear to their teeth due to blown sand entering their food, dental attrition is not as accurate an ageing method for Nekht-Ankh as it would be for other populations. All epiphyses except the junction between the manubrium and the sternal body were fully fused, indicating that he was over thirty when he died. Cameron states that the coronal and sagittal sutures were obliterated on the interior surface of the cranium.⁴⁹¹ The majority of the cranial sutures were fusing but still very visible on the external table of the cranium, but it was not possible to assess the state of the sutures on the internal table of the cranium, due to the restricted access through the foramen magnum by the tools available. Nekht-Ankh appears to be a mature adult, but due to the curation of the mummy (i.e., wired into anatomical position), it is not possible to more accurately define an age category.



Figure 6.8: Nekht-Ankh's dentition, displaying his erupted third molars and heavily worn teeth. Photo by author.

Nekht-Ankh's skull displays a flattening of the area between the foramen magnum and the external occipital protuberance (**Figure 6.9**). Whether this is due to castration is brought into question, as there is no visible difference in this area between

⁴⁹⁰ (Brothwell, 1989)

⁴⁹¹ (Cameron, 1910)

Nekht-Ankh and Khnum-Nekht.⁴⁹² When the mummy was initially unwrapped, the upper right lateral incisor was missing. As is visible in **Figures 6.8 & 6.9**, more teeth have come loose from the skull since the unwrapping. The mandible is small and square, with a prominent mental eminence and an almost ninety degree gonial angle. The body of the mandibular ramus is short and wide, with a shallow notch. The maxilla is slightly prognathic, though Cameron originally described Nekht-Ankh's face as extremely orthognous (**Figure 6.9**). The nasal bones are very straight and long, the nasal aperture is wide and tall, and there is no evidence of the suture between the two maxillary bones. The superciliary ridges are fairly well developed, but the supraorbital margin is sharp. The zygomatic arches are very gracile and delicate, and do not extend beyond the external auditory meatus. The mastoid processes are short and anteriorly directed, and there is little to no suggestion of the nuchal crest or external occipital protuberances. All of these cranial features suggest a very gracile, feminine individual.



Figure 6.9: Detailed anterior and left lateral views of the skull of Nekht-Ankh. Photo by author.

The entire skeleton is very gracile, with no evidence for major development of the muscle attachment sites and no particular elongation of the long bones. There is evidence of osteoporosis throughout the skeleton, most obviously in the thinness of the iliac fossae, the bodies of the scapulae, and the porosity of the vertebral bodies. The pelvis is very masculine in appearance, with a narrow subpubic angle and very narrow sciatic notches (**Figure 6.10**). The ischiopubic rami are neither thick nor thin, and the

⁴⁹² (Cameron, 1910)

obturator foramina are “D”-shaped. The acetabulae are wide and shallow, placed semi-anteriorly on the pelvic girdle. The true and false pelvis are both very vertical and narrow, with very little splay of the ilia. The sacrum is not particularly curved, leaving a fairly broad pelvic outlet. Overall, Nekht-Ankh’s appearance is very gracile and slightly feminine, but the majority of his secondary sex markers appear masculine. It is possible that he was a castrate, but likely that he is a postpubertal castrate rather than prepubertal.

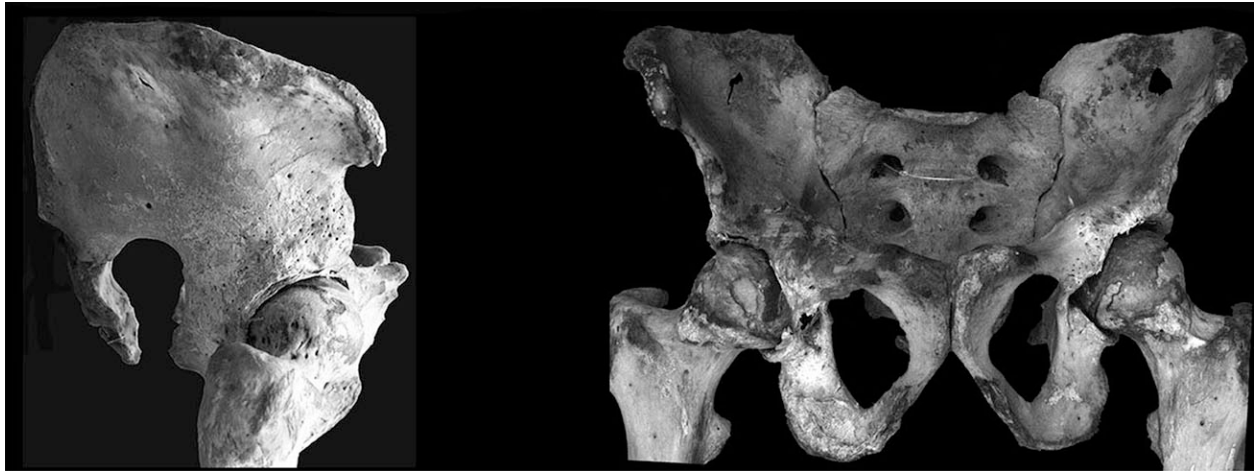


Figure 6.10: Detailed anterior and right lateral views of the pelvis of Nekht-Ankh, displaying the shape of the subpubic angle and sciatic notch. Photo by author.

6.1.1.1.3 The Eng Eunuchs and the Tandler and Grosz Castrate

Images of the skulls of the Tandler and Grosz castrate and the two Ming dynasty eunuchs examined by Eng were included in their respective publications,⁴⁹³ allowing them to be examined and discussed here. Eunuch M1 (**Figure 6.11**) has a sloping forehead; no obvious superciliary ridge; slightly rounded supraorbital margins; rectangular orbits; low, short nasal bones; and fairly orthognous maxillary and mandibular dentition. The mental eminence of M1 is not particularly pronounced, and the mandibular body is solid but relatively shallow, with a slightly obtuse gonial angle, slight gonial flaring, and a wide mandibular ramus with a relatively sharp notch. The nasal aperture is taller than it is wide, with a sharp ridge inferior to the aperture, running along the join between the two maxillae, which appear to have fully fused. The zygomae are not particularly pronounced, though the delicate zygomatic arches stop just above the external auditory meatus. The mastoid process appears short and slightly anteriorly

⁴⁹³ (Eng et al., 2010; Tandler and Grosz, 1909)

pointed, and there is some suggestion of the external occipital protuberance. The posterior portion of the cranium is very short and rounded.

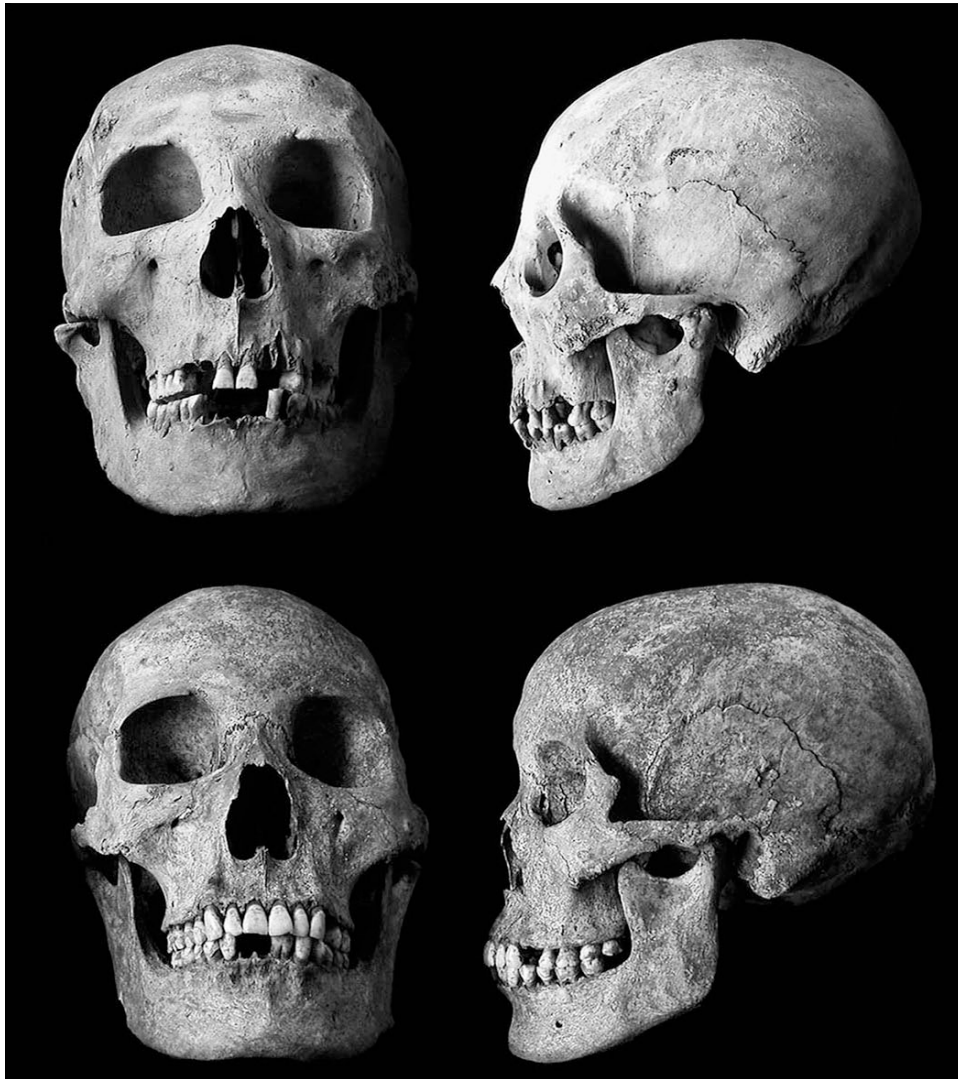


Figure 6.11: Detailed anterior and left lateral views of the skulls of the Eng eunuchs, M1 (upper) and M2 (lower). (Image from Eng et al., 2010)

Eunuch M2's skull (**Figure 6.11**) has a more vertical, feminine-appearing craniofacial aspect, with an upright forehead, slight superciliary ridges, what appear to be sharp supraorbital margins, rectangular orbits, short and narrow nasal bones which form a concave curve where they articulate with the frontal bone, a tall and wide nasal aperture, and a slightly prognathic maxilla with a ridge of possibly open fusion between the two maxillary bones. The mandible has a slightly prognathic dentition, a somewhat pronounced mental eminence, a fairly heavy body, an almost ninety degree gonial angle, slight gonial flaring, and a wide mandibular ramus with a very shallow notch. The

zygoma are lighter than those of eunuch M1, though the zygomatic arches appear to be about the same weight (delicate and thin) and stop slightly beyond the external auditory meatus. The mastoid processes are extremely short and appear to angle anteriorly. The posterior cranium possesses a very ovoid shape, with a suggestion of a nuchal crest and possibly the external occipital protuberance.

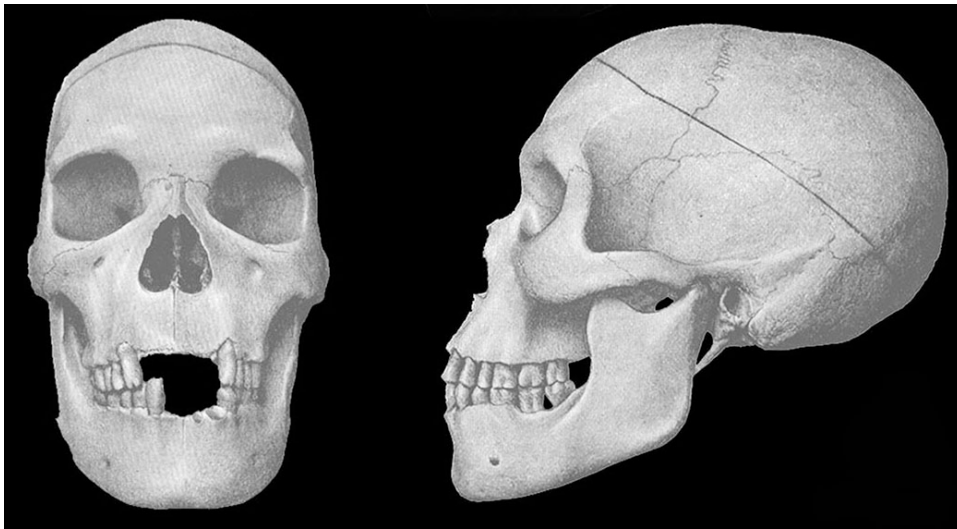


Figure 6.12: Detailed anterior and left lateral views of the skull of the Tandler and Grosz castrate. (Image taken from Tandler and Grosz, 1909)

The Tandler and Grosz castrate's skull (**Figure 6.12**) has a very prognathic facial aspect, with a sloping forehead, developed superciliary ridges, slightly rounded supraorbital margins, very narrow and short nasal bones which form a deeply concave curve where they articulate to the frontal bone, a short but wide nasal aperture, and a prognathic maxilla with open fusion between the maxillary bones. The mandible also possesses somewhat prognathic dentition, a definite mental eminence, a deep body, a slightly obtuse gonial angle but apparently little gonial flaring, and a short, wide mandibular body with a very shallow notch. The zygoma are small and narrow, though the zygomatic arches seem somewhat robust and appear to extend slightly beyond the external auditory meatus. The mastoid process is very short and anteriorly angled. The posterior portion of the cranium is ovoid in shape and does not appear to possess either a nuchal crest or a pronounced external occipital protuberance.

The pelvic girdles of the two Ming dynasty eunuchs were not included in the article, so it is not possible to discuss them here. The true pelvis of the Tandler and Grosz skeleton is vertical but broad, with a masculine, v-shaped subpubic angle but a

wide, indeterminate or feminine sciatic notch (**Figure 6.13**). It has a wide, broad pelvic inlet, forming an oval. The obturator foramina have a definite “D”-shape, indicating that the pubis and ischium have lengthened, which contributes to the broader shape of the pelvic inlet, though the curve of the sacrum greatly narrows the shape of the outlet. The acetabulae are also situated very anteriorly, and the ilia flare laterally and posteriorly, but at a more vertical angle than those of the Lyon castrate.

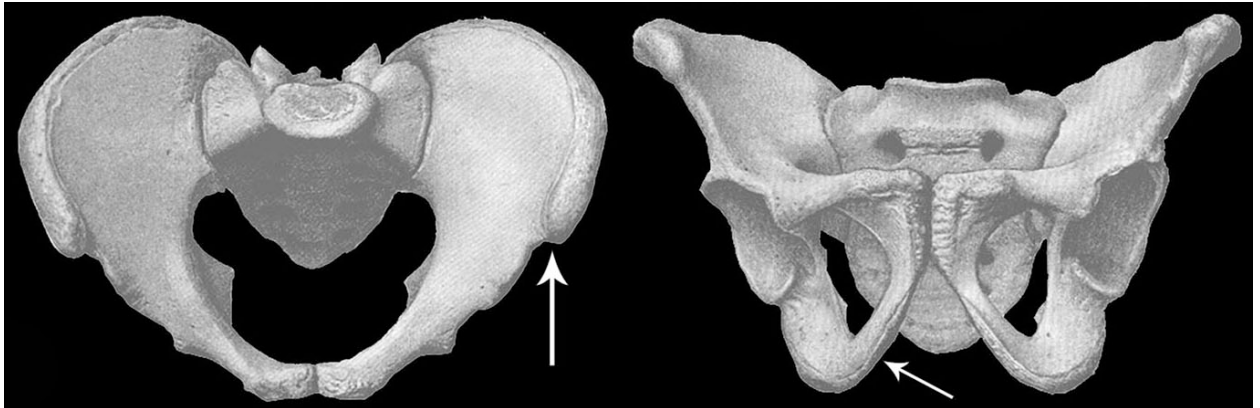


Figure 6.13: Detailed superior and anterior views of the pelvis of the Tandler and Grosz castrate, displaying the shape of the subpubic angle and sciatic notch and with arrows showing the open epiphyses. (Image taken from Tandler and Grosz, 1909)

6.1.1.1.4 Comparisons of Skulls and Pelves

When placed in a series, it is possible to detect similarities and differences among the skulls of the five castrates examined above (**Figure 6.14**). As both Eng castrates are Chinese, the Tandler and Grosz and Lyon castrate are African, and Nekht-Ankh is either Caucasian or Caucasian-African mixed, it should be possible to determine whether any changes to the skulls of the castrates might be due to ancestry. Both Chinese castrates have very straight, slightly delicate zygomatic arches and relatively orthognathous faces (**Figure 6.14, a & b**), but the mandibular angle on M2 (**6.14b**) is much more square than that of M1 (**6.14a**). In addition, M2 displays some degree of mandibular and maxillary prognathism, perhaps as a result of delayed fusion in the craniofacial region. The cranium of M2 is also much more ovoid in appearance as a result of its narrow depth and long length. As M1 is probably a postpubertal castrate and M2 is probably a prepubertal castrate,⁴⁹⁴ it may be that the majority of the differences between M1 and M2 are due to the difference in timing of their castrations, with M1’s skull more closely resembling that

⁴⁹⁴ (Eng et al., 2010)

of an adult Chinese male. The Lyon castrate exhibits a similar craniofacial morphology to that of the Zanzibar-born Tandler and Grosz skeleton (**Figure 6.14, c & d**), with heavy, square mandibles and prognathic dentition.⁴⁹⁵ Both skulls share the ovoid shape M2 displays, with long, narrow crania. The Lyon castrate's zygomatic arches are very thin and delicate (**6.14c**), but those of the Tandler and Grosz castrate are more pronounced (**6.14d**). However, both the Tandler and Grosz castrate's and the Lyon castrate's zygomatic arches are very curvilinear, with a small superiorly oriented arch just past the zygomaticotemporal suture. Nekht-Ankh appears to share characteristics of both the Chinese and African castrates (**Figure 6.14e**), with a fairly orthognathous face, except for his prognathic dentition, delicate but straight zygomatic arches, and ovoid cranium.

Aside from changes related to ancestry, there are some changes to the crania that are likely linked to age of castration. Eng's eunuch M2 (**6.14b**), the Lyon castrate (**6.14c**), and the Tandler and Grosz castrate (**6.14d**) are all known to be prepubertal castrates.⁴⁹⁶ As Eng's eunuch M1 (**6.14a**) was determined to be a postpubertal castrate,⁴⁹⁷ and Nekht-Ankh (**6.14e**) is likely a postpubertal castrate, likely differences between the two castration timings can be noted. The three prepubertal castrates possess heavy mandibles, with square gonial angles and wide, thick mandibular rami with shallow notches. While the two African castrates possess wider rami than M2, it seems that the formation of the mandibular body is affected by prepubertal castration. The distortion of the mandibles could be caused by repetitive, strained chewing, either of food or some other material, or some other form of muscular strain on the mandible, but as none of their teeth showed particularly heavy wear, nor did their vertebrae or shoulder girdles show signs of developed muscular attachments, this seems unlikely. All three prepubertal castrates also possess varying degrees of dental prognathism, though it is the least noticeable in M2. The Tandler and Grosz castrate and M2 possess very concave nasal roots, where the nasal bones join to the frontal bone, but as the Lyon castrate does not appear to display this characteristic, it may not be associated with castration. The zygomatic bones of all three prepubertal castrates are very square in shape, and in the case of the Lyon castrate and M2, seem to project slightly anterior to the maxillary bones. Possibly due to a lack of

⁴⁹⁵ (Tandler and Grosz, 1909: 44–45)

⁴⁹⁶ (Eng et al., 2010; Tandler and Grosz, 1909)

⁴⁹⁷ (Eng et al., 2010)

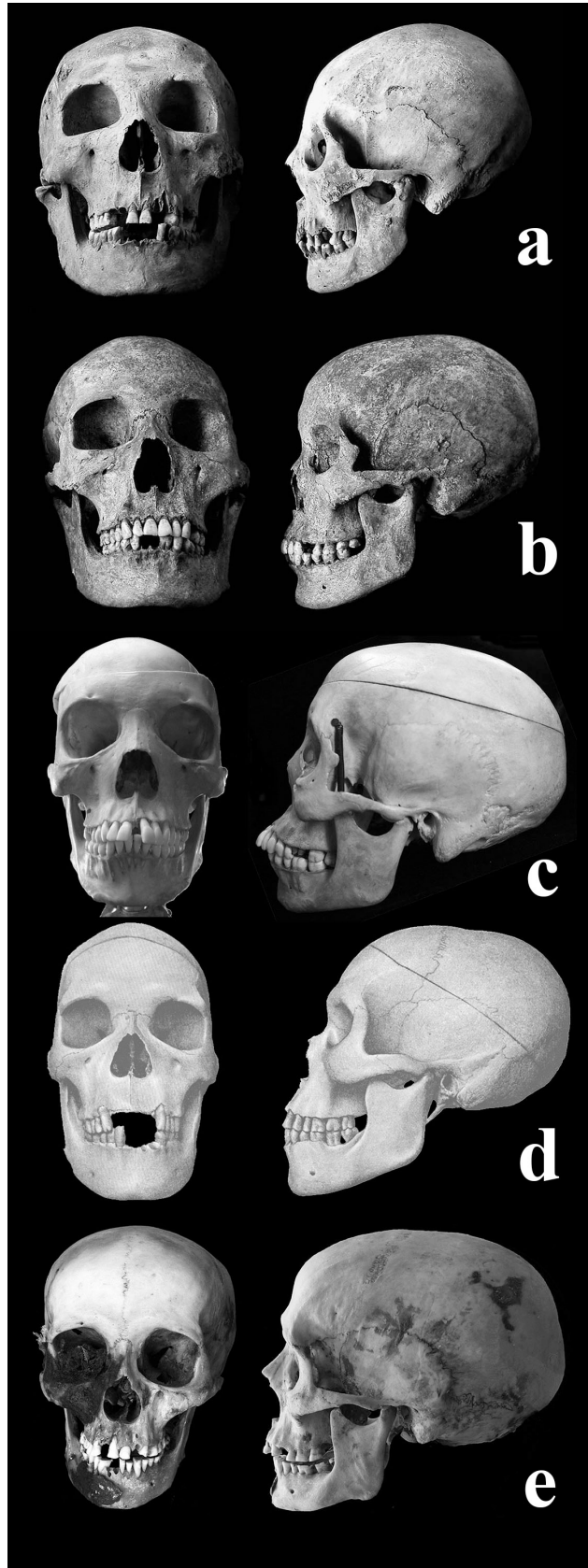


Figure 6.14: Comparison of the skulls of (a) Eng M1, (b) Eng M2 (2010), (c) Lyon, (d) Tandler and Grosz (1909), and (e) Nekht-Ankh showing craniofacial changes due to castration (a, b, and d taken from their relevant publications; c and e photographs by author).

hormones and a failure of the subsequent widening of the face (as mentioned in Chapter 5), all three prepubertal castrates have tall, narrow faces.

The prepubertal castrates and Nekht-Ankh share long, narrow, ovoid crania, but whether this is a symptom of castration is unclear. Nekht-Ankh and M1 share fairly normal mandibles, though their mandibular rami are somewhat thick and may possess more shallow notches than normal. Nekht-Ankh has a slightly prognathic dentition and a very upright forehead, while M1 does not seem to have a very pronounced dentition and has a very sloped forehead, both of which features may be more related to ancestry than castration. Two features that are shared by all five individuals are ovoid-rectangular orbits, and a clearly defined zygomaticotemporal suture, but as this suture normally closes in the eighth decade of life,⁴⁹⁸ this is most likely not a symptom of castration.

As the Eng publication did not include images of the eunuchs' pelves, it is only possible to compare the pelves of the Lyon castrate (**Figure 6.15a**), the Tandler and Grosz castrate (**6.15b**), and Nekht-Ankh (**6.15c**). As the Lyon castrate and Tandler and Grosz castrate are both prepubertal castrates and Africans and Nekht-Ankh is both a postpubertal castrate and either Caucasian or mixed, determining whether changes to the pelves are due to castration or differences in ancestry will be difficult. Both prepubertal pelves display lateral and posterior flaring of the ilia, though the Tandler and Grosz castrate's ilia flare at a more vertical angle than those of the Lyon castrate. This flaring creates a "heart" shape in the superior view of both pelves, though the Tandler and Grosz castrate is not as extreme. Lines of epiphyseal fusion are visible on both the iliac crests and the ischia of both pelves. Due to the outward flare of the ilia, both prepubertal pelves appear short and wide, while Nekht-Ankh's pelvis appears relatively narrow and vertical, as his ilia do not flare very laterally. All three pelves appear very masculine in the subpubic angle and sciatic notch, though all three have fairly feminine obturator foramina, and all three castrates' acetabulae are situated very anteriorly. It appears that prepubertal castration does not erase all sexually dimorphic features of the male pelvis, as at least two of the features standardly used to sex skeletons (the sciatic notch and subpubic angle)⁴⁹⁹ are still clearly masculine. Combined with the unusual flaring of the ilia, the placement of the acetabulae, and the clearly visible fusion lines, castrate pelves appear to have some distinctive characteristics.

⁴⁹⁸ (Rogers et al., 2007)

⁴⁹⁹ (Brickley and McKinley, 2004; Buikstra and Ubelaker, 1994)

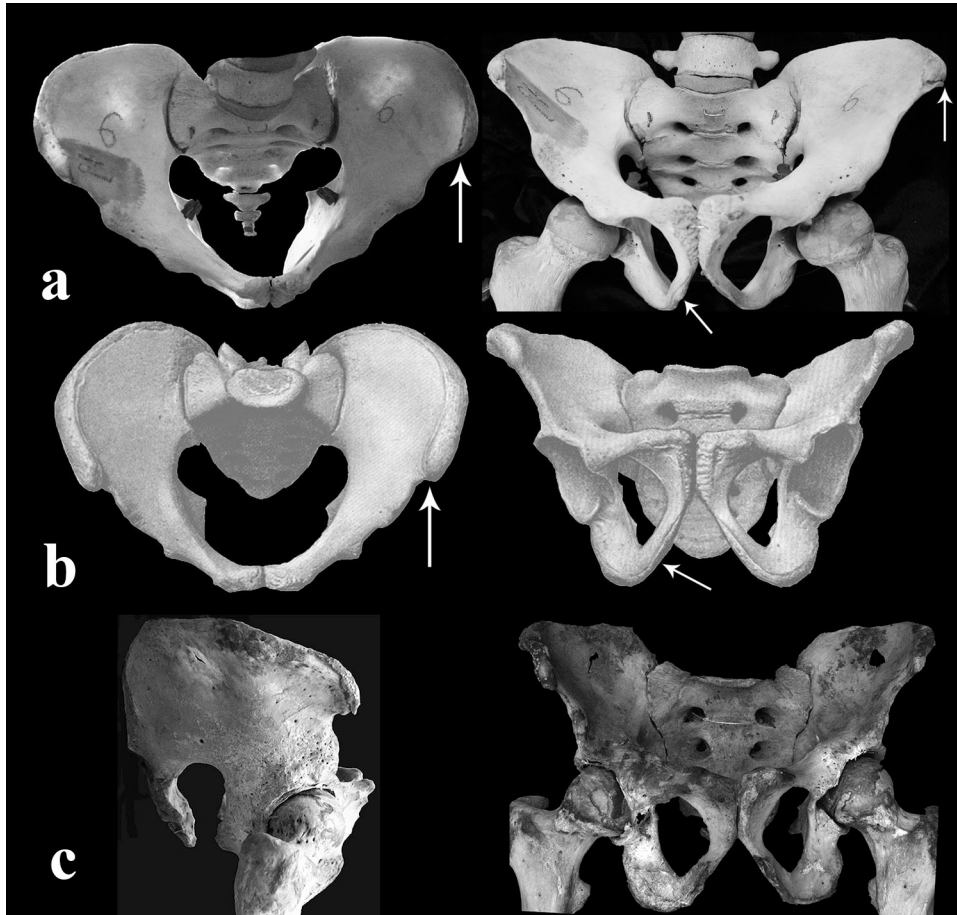


Figure 6.15: Comparison of the superior and anterior views of the pelvic girdles of (a) the Lyon castrate and (b) the Tandler and Grosz castrate (1909) and lateral and anterior views of (c) Nekht-Ankh, displaying the open epiphyses (arrows) and the shape of the true pelvis, pelvic inlet, ilia, subpubic angle, and sciatic notches.

6.1.1.2 Metric Analysis

There are a number of morphological changes to the skeleton caused by castration (as discussed in Chapter 5 and the previous sections of this chapter), but very few castrate skeletons have been identified in European, Western Asian, and North African burial populations, where one would expect to find a large number. Therefore, it appears that morphological change is not enough to detect castrate skeletons. However, due to the extra growth of the long bones of the skeleton caused by delayed epiphyseal fusion, it is possible to separate at least some castrates from the wider population through the analysis of long bone measurements, as shown here.

Though the visual aspect of disproportion disappears when the Lyon skeleton is laid out in anatomical position, disproportion can still be detected in the measurements of the skeleton. When zooarchaeologists wish to determine sex distributions within populations, they plot length versus breadth ratios of animal long bones to separate males,

females, and castrates in faunal assemblages.⁵⁰⁰ This method is applied to the Lyon castrate, the Judd data, and the FORDISC dataset here.⁵⁰¹

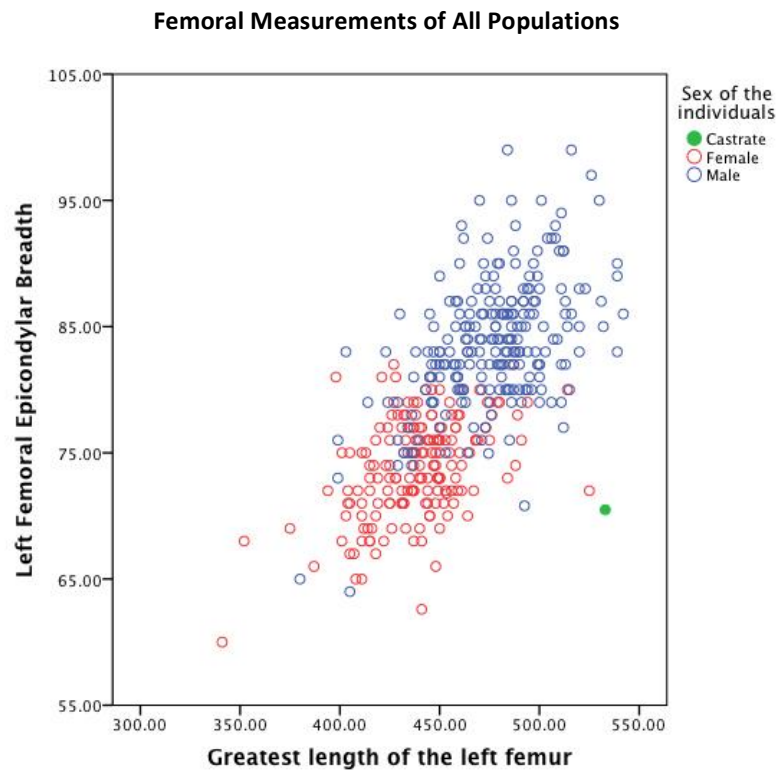


Figure 6.16: Comparison of femoral length versus breadth of the Lyon castrate against those of the total FORDISC population (measurements in mm).

When the greatest length of the femur is graphed versus femoral distal breadth, the FORDISC population shows a range of measurements in a generally linear distribution. Compared to this range, the Lyon castrate stands out as having a longer but thinner femur than most of the population (**Figure 6.16**). There are some males with femora as long as or slightly longer than his, and some females in the same or narrower breadth range as him, just as there are overlaps between the male and female portions of the population, but the combination of length and breadth measurements sets him apart from the “normal” range of variation in the population. The Lyon castrate’s status as an outlier, especially in relation to the males, is demonstrated also when comparing the skeleton to only the Africans in the FORDISC database and to Judd’s data, as he is

⁵⁰⁰ (Armitage and Clutton-Brock, 1976; Davis, 2000; De Cupere et al., 2005)

⁵⁰¹ (Welsby, 2001)

shown to have a distinctly longer femur than the majority of males, while the distal breadth is on the low end for a female (**Figure 6.17**).

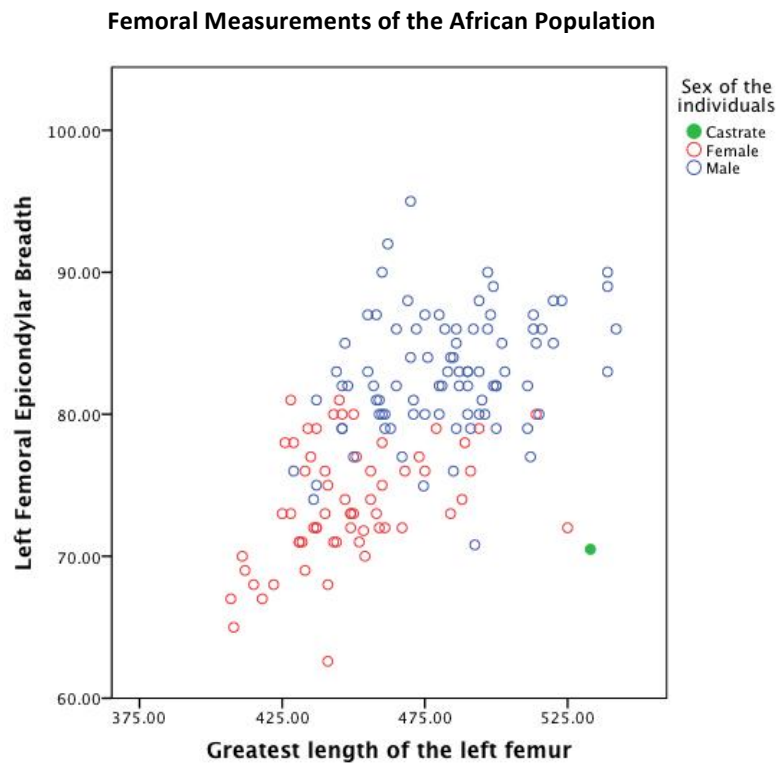


Figure 6.17: Comparison of the femur length versus breadth of the Lyon castrate against those of the FORDISC African population (measurements in mm).

When graphing the tibia, both the proximal and distal breadths versus the length show that the Lyon castrate falls outside the normal range of the population (**Figure 6.18**). He lies between the male and female portions of the population in breadth, but shares length with only a few males. The humerus shows a similar pattern to the tibia, but does not differ from the majority to such a large extent. This may be because daily physical activities the castrate performed influenced the breadth of the humeral epicondyles. However, it does suggest that the elongation of the long bones is consistent in both the upper and lower limbs of castrates, and that either could potentially be used to differentiate castrates within a skeletal population (**Figure 6.19**).

Tibial Measurements of the African Population

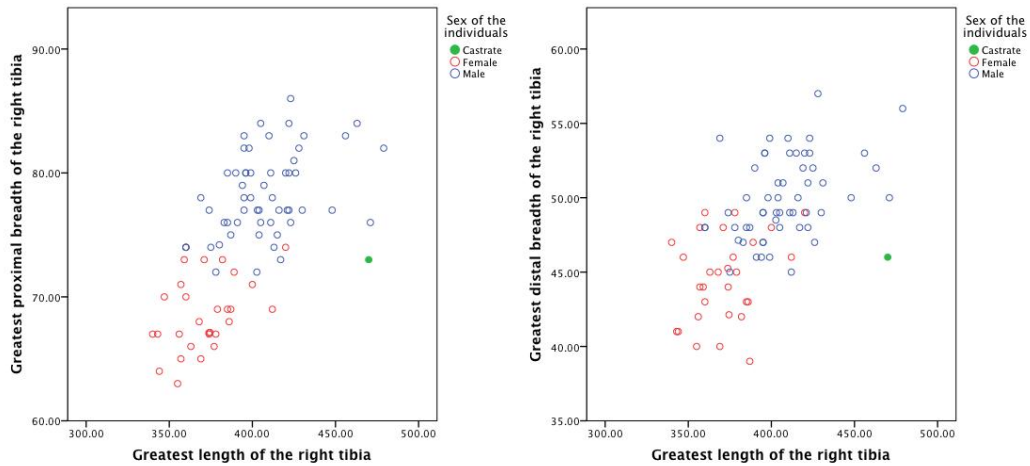


Figure 6.18: Comparison of the tibia length versus proximal (left) and distal (right) breadths of the Lyon castrate against those of the FORDISC African population (measurements in mm).

Humeral Measurements of the African Population

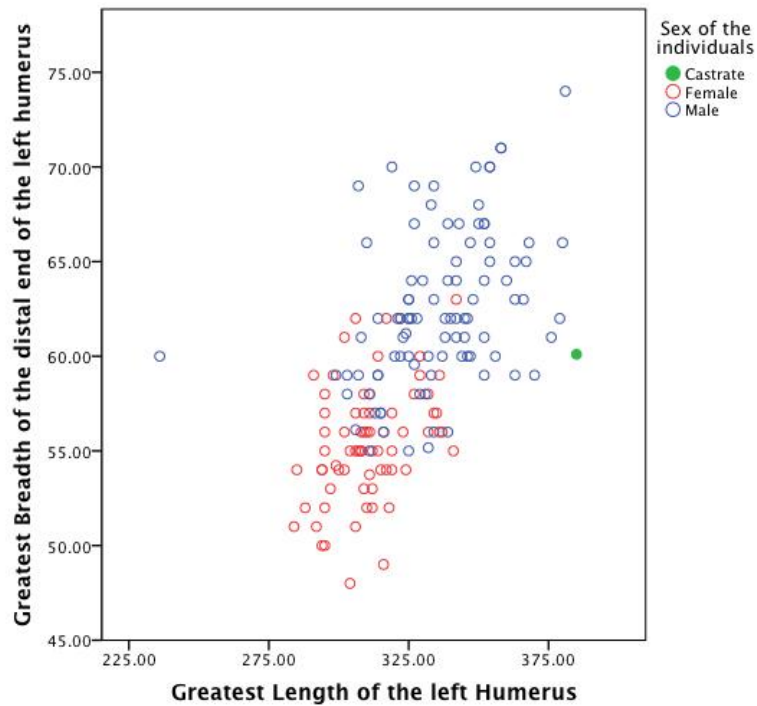


Figure 6.19: Comparison of the humerus length versus breadth of the Lyon castrate against those of the FORDISC African population (measurements in mm).

The closest possible comparative collection for Nekht-Ankh has been taken from a dataset of skeletal measurements obtained from the radiographs of Egyptian mummies from the Late Intermediate to Roman periods housed in the National Museum of Antiquities in Leiden, the Netherlands and the measurements recorded for Nekht-Ankh's

brother, Khnum-Nekht in the original Murray publication.⁵⁰² As neither dataset contained breadth measurements, only the length ratios between bones could be compared. The dataset of the Leiden mummies was small (consisting of only thirty-one complete mummies), and the age, sex, and complete, measurable long bones ranged widely. As one of the major questions surrounding Nekht-Ankh is his status as a castrate, his positioning relative to other members of the dataset is particularly important.

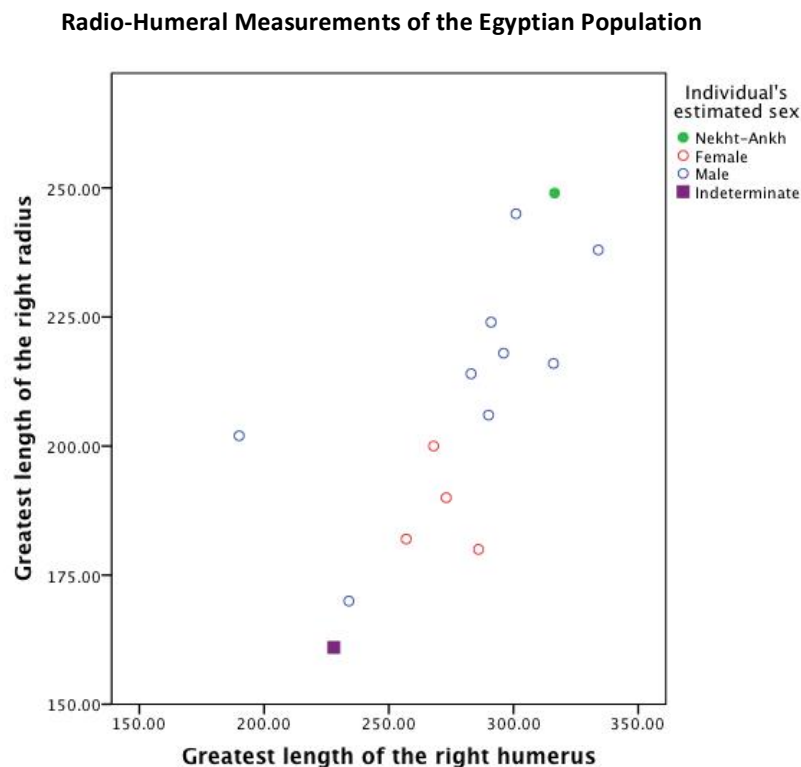


Figure 6.20: Comparison of the length of the radius versus the length of the humerus of Nekht-Ankh versus the Egyptian population (measurements in mm) (Comparative data from Cameron, 1910 and Raven and Taconis, 2005).

In the graph of radial versus humeral length (**Figure 6.20**), there is a definite linear trend, with Nekht-Ankh and Khnum-Nekht at the very upper end of radial and humeral length, though there are individuals with longer humeri than Nekht-Ankh. The two males and one indeterminate individual at the lower end of the humeral measurements are teenagers and likely had not achieved their full growth at the time they died.

⁵⁰² (Cameron, 1910; Raven and Taconis, 2005)

Humero-Femoral Measurements of the Egyptian Population

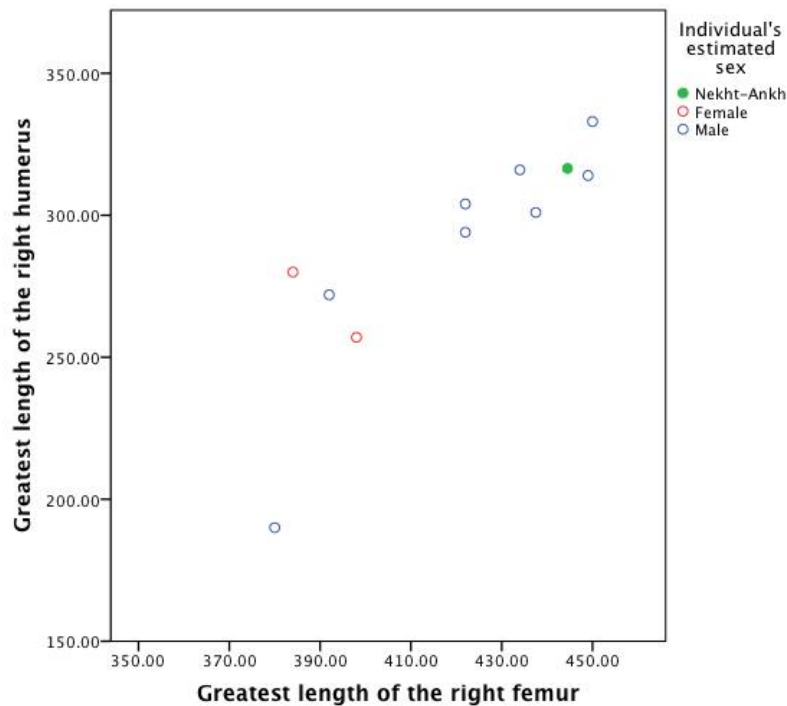


Figure 6.21: Comparison of the humero-femoral ratio of Nekht-Ankh versus the Egyptian population (measurements in mm) (Comparative data from Cameron, 1910 and Raven and Taconis, 2005).

The graph of humeral versus femoral length (**Figure 6.21**), shows some linear trending, but does not separate Nekht-Ankh from the general male Egyptian population as well as the previous comparison. He is positioned at the high end of both femoral and humeral measurements, but the rest of the male population solidly surrounds him. The male at the extreme low end of both femoral and humeral length is again an adolescent and not fully grown. In the same manner, the femoral-tibial graph (**Figure 6.22**) does not seem to separate Nekht-Ankh from the general male Egyptian population very well. He does have the longest tibia, but he does not possess the longest femur. Again, the individuals with the smallest measurements are adolescents. The inability to separate Nekht-Ankh from the general male Egyptian population and his lack of open epiphyses suggest that, if Nekht-Ankh is a castrate, castration must have happened postpubertally, as there are not enough strong indicators of prepubertal changes to his skeleton. As he is positioned at the upper extremity of the male Egyptian population measurements in terms of long bone lengths, he may have been castrated postpubertally, but before all his epiphyses had fused, allowing the slight elongation of his long bones.

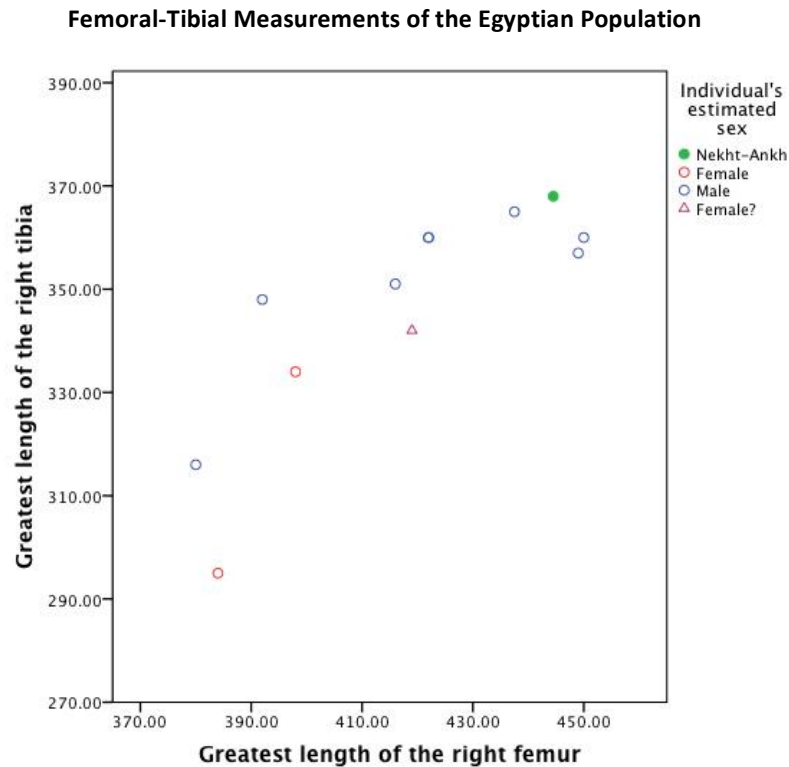


Figure 6.22: Comparison of the femoral-tibial ratio of Nekht-Ankh versus the Egyptian population (measurements in mm) (Comparative data from Cameron, 1910 and Raven and Taconis, 2005).

6.1.2 Animals

6.1.2.1 Morphological Analysis

There are few castrate animal skeletons available that have not come from previously published, targeted studies of castration (such as those from Davis' examination of Shetland sheep⁵⁰³). The largest study of castrated animals which has published long bone data was performed on sheep in the United Kingdom.⁵⁰⁴ A collection of Shetland wether and ram skeletons was acquired over several years from a single farm on Hoy by the Ancient Monuments Laboratory and was compared to the skeletons of Shetland ewes taken from a neighbouring farm.

Tooth eruption was taken to be a reliable indicator of age as there was little difference between rams and wethers despite the wethers exhibiting delayed epiphyseal fusion. This is consistent with the observations regarding tooth eruption in human skeletal remains described above and anthropological studies of castrates.⁵⁰⁵ Davis noted

⁵⁰³ (Davis, 2000)

⁵⁰⁴ (Davis, 2000)

⁵⁰⁵ (Pittard, 1934)

that previous studies of wethers had indicated that fusion times for castrates were consistent irrespective of breed, unlike the fusion times for male and female sheep.⁵⁰⁶

6.1.2.2 Metric Analysis

Davis shows that long bone length versus breadth measurements can be used to separate the sexes in sheep, which studies concerning other domestic agricultural animals substantiate to varying degrees.⁵⁰⁷ The long bones of castrated sheep are longer than those of males or females, while widths hover between male and female values, sometimes overlapping both categories (**Figure 6.23**).⁵⁰⁸ This makes the application of length versus breadth examinations of animal long bones of somewhat limited use to zooarchaeologists, but can be used to indicate the possible presence of castrates in herds. The least amount of overlap between males and females and castrates is seen in the metacarpal measurements (**Figure 6.24**). If the shaft diameter measurements of the long bones are available, graphing the femur length versus the shaft diameter (**Figure 6.25**) sets castrates apart even better than the use of the breadth of the epiphyses.

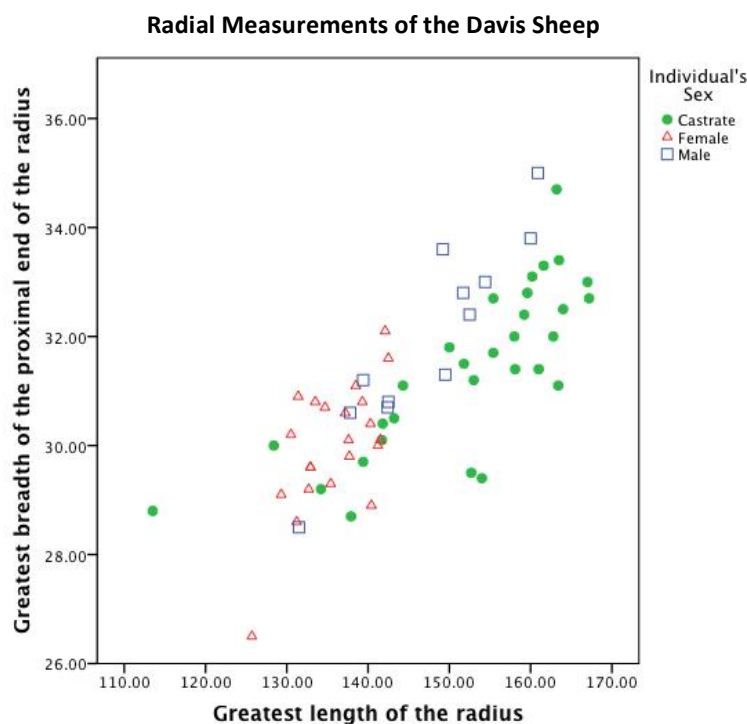


Figure 6.23: Comparison of the length to breadth (in mm) of the Davis sheep radii, displaying a similar distribution of castrates to males and females (data from Davis, 2000).

⁵⁰⁶ (Davis, 2000)

⁵⁰⁷ (Armitage and Clutton-Brock, 1976)

⁵⁰⁸ (Davis, 2000)

Metacarpal Measurements of the Davis Sheep

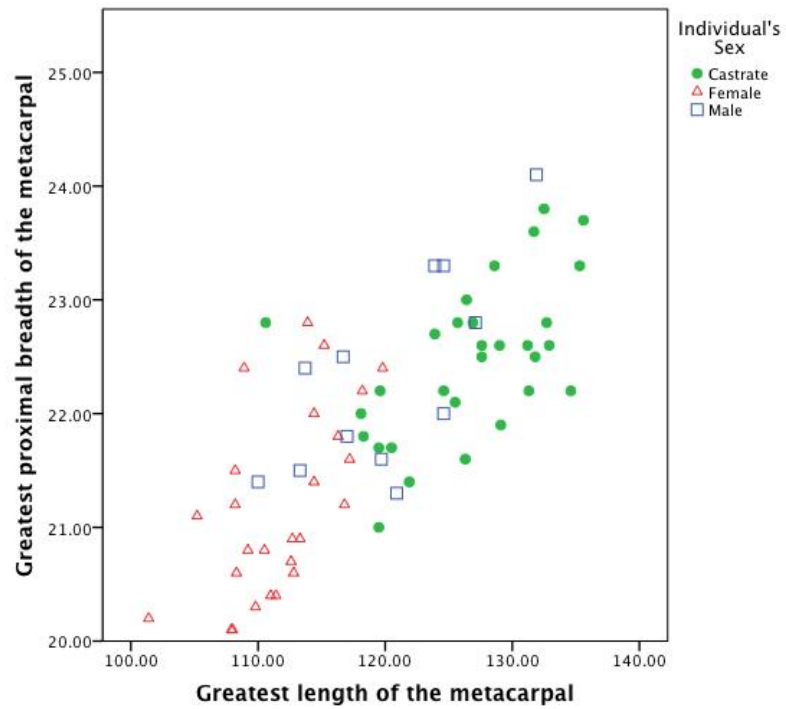


Figure 6.24: Metacarpal length versus proximal breadth (in mm) in the Davis sheep, showing the best separation amongst the three groups (data from Davis, 2000).

Femoral Measurements of the Davis Sheep

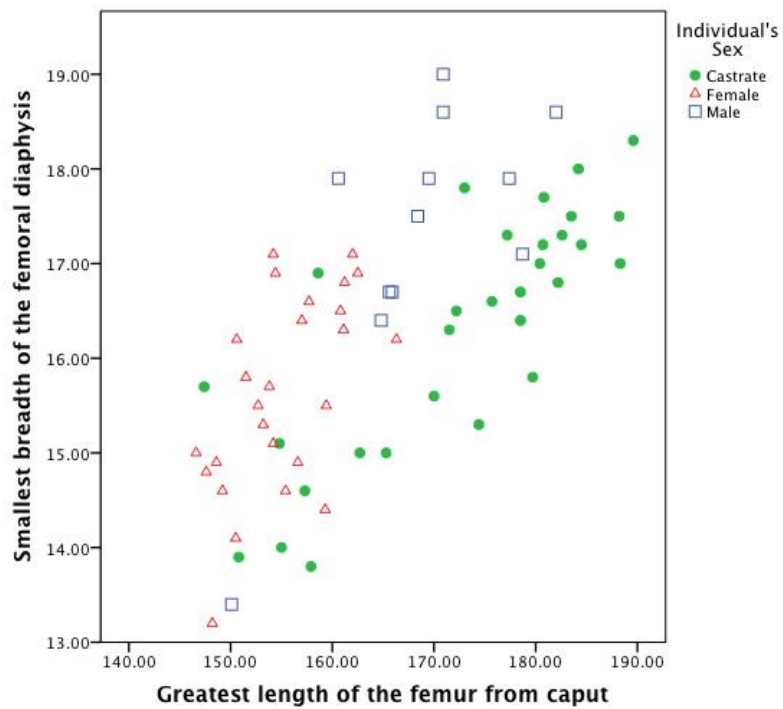


Figure 6.25: Comparison of the length of the femur to the shaft diameter (in mm), showing the clear separation of the castrates (measurements in mm) (data from Davis, 2000).

6.2 Results of Anthropometric Analysis

6.2.1 Humans

6.2.1.1 Metric Analysis

As the major points of the morphological analysis were covered in Chapter Five, only the metric analysis of the human anthropometric data set will be discussed here. The anthropometric measurement of pubic symphysis height (PSH) gives the overall lower limb length in a standing individual, measured from the floor to the upper edge of the pubic symphysis. In order to assess the effect of the age of castration on the development and configuration of the skeleton, the castrates were divided into three age groups based upon their reported ages of castration: prepubertal (<13), midpubertal (14-18), and postpubertal (19+) castration. Anticipated differences between prepubertal castrates and postpubertal castrates were visible (**Figure 6.26**).

Comparison of Pubic Symphysis Height and Stature in the Castrate Population

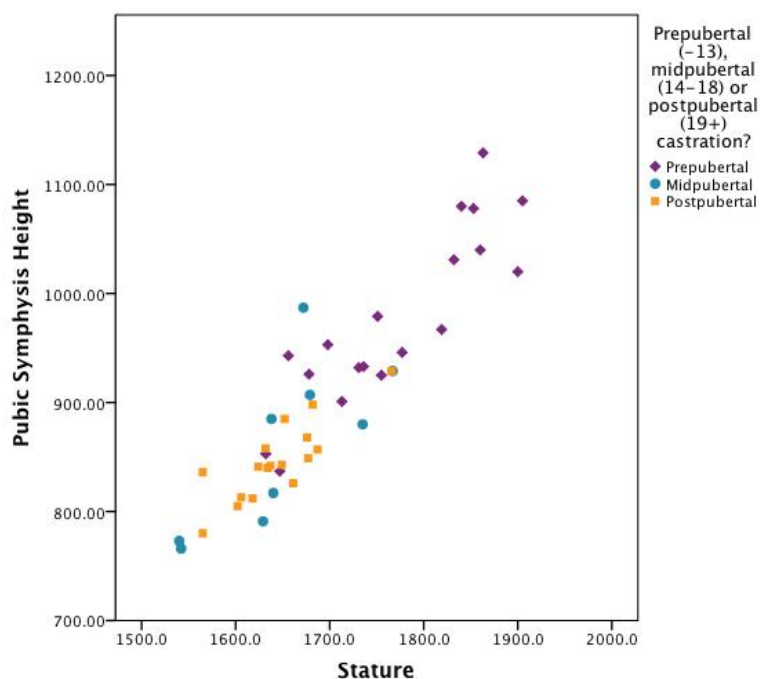


Figure 6.26: Comparison of the stature to pubic symphysis height (in mm) in the castrates, showing the differences between prepubertal, midpubertal, and postpubertal castrates (Synthesized and graphed by author from data taken from Tandler and Grosz, 1910; Wagenseil, 1933, 1927).

Some midpubertal castrates show the same development of their stature and pubic symphysis height as prepubertal castrates, indicating that the growth of the long

bones which contribute the most to stature, i.e., the tibia, fibula, and femur, is affected by castration both before and during puberty. This coincides with Wagenseil and Pittard's reports that those castrated at a young age showed the most growth in stature, but that those castrated before their 20s could still grow quite tall.⁵⁰⁹ That growth in stature is mostly contributed by the legs is demonstrated in **Figure 6.27**, which shows the distribution of pubic symphysis height according to age of castration. Almost all of the tallest individuals were castrated pre- or midpubertally. Not all individuals with high pubic symphysis height were prepubertally castrated. However, that the largest number of those with pubic symphysis heights over 90 cm are pre- or midpubertal castrates indicates that in order to consistently achieve these lengths, hormonal activity must be unusual.

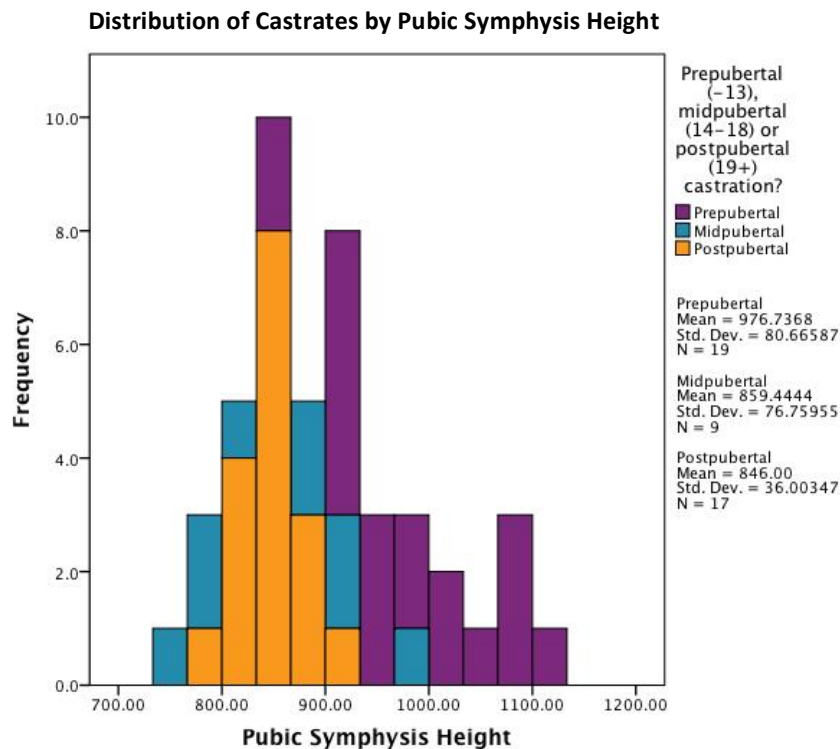


Figure 6.27: Division of castrates according to pubic symphysis height (in mm), demonstrating that castration before or during puberty creates individuals with longer lower limbs than those castrated after puberty (distribution created by author from data collated from Tandler and Grosz, 1910; Wagenseil, 1933, 1927).

The large contribution to lower leg length seen in pre- and midpubertal castrates is due to the delay of fusion beyond the 'normal' fusion times of the epiphyses of the bones of the lower leg. The bones of the lower leg begin fusion during puberty, the point

⁵⁰⁹ (Pittard, 1934; Wagenseil, 1933a, 1927)

at which an individual's total growth period is nearing its end. The femoral head, distal tibia, and distal fibula are usually completely fused by twenty years, the distal femur and proximal fibula follow at twenty-one to twenty-two years, and the proximal tibia is normally fused by twenty-two to twenty-three years of age.⁵¹⁰ Growth and puberty can be delayed by poor nutrition or chronic illness, leaving the epiphyses open. Individuals who suffer malnutrition and illness tend to have shorter stature, due to the need for 'catch-up' growth and a shorter pubertal period.⁵¹¹ Pre- and midpubertal castrates who experience delayed fusion without accompanying illness or malnutrition therefore have a period of long, slow, steady growth, allowing their long bones to achieve unusual lengths. As postpubertal castrates are castrated after the majority of bone fusion should have occurred, there is less chance of any delayed epiphyseal fusion contributing to extra length in the long bones.



Figure 6.28: Comparison of stature to pubic symphysis height (in mm) for all ancestry groups, showing the separation between the castrates and the males and females (castrate data from Wagenseil, 1933a, 1927).

⁵¹⁰ (McKern and Stewart, 1957; Scheuer and Black, 2000)

⁵¹¹ (Trowbridge et al., 1987; Yeo, 2005)

There is a great difference between castrates and non-castrates in lower limb length, as can be seen in **Figure 6.28**. While most of the non-castrate population follows the same linear distribution range with considerable overlap between males and females, castrates vary widely in lower limb length. The pre- and midpubertal castrates generally have longer lower limb versus stature values than most of the males or females, while the postpubertal castrates, though exhibiting longer lower limb versus stature, overlap the upper values seen in males and females. When examined by ancestry group, this pattern becomes even more obvious. Asian castrates are almost all much longer-legged versus stature than either their male or female counterparts (**Figure 6.29**). Similar results are seen when African castrates are compared only to their counterparts and when European castrates are compared only to their counterparts (**Figure 6.30**).

Comparison of Pubic Symphysis Height and Stature in All Populations

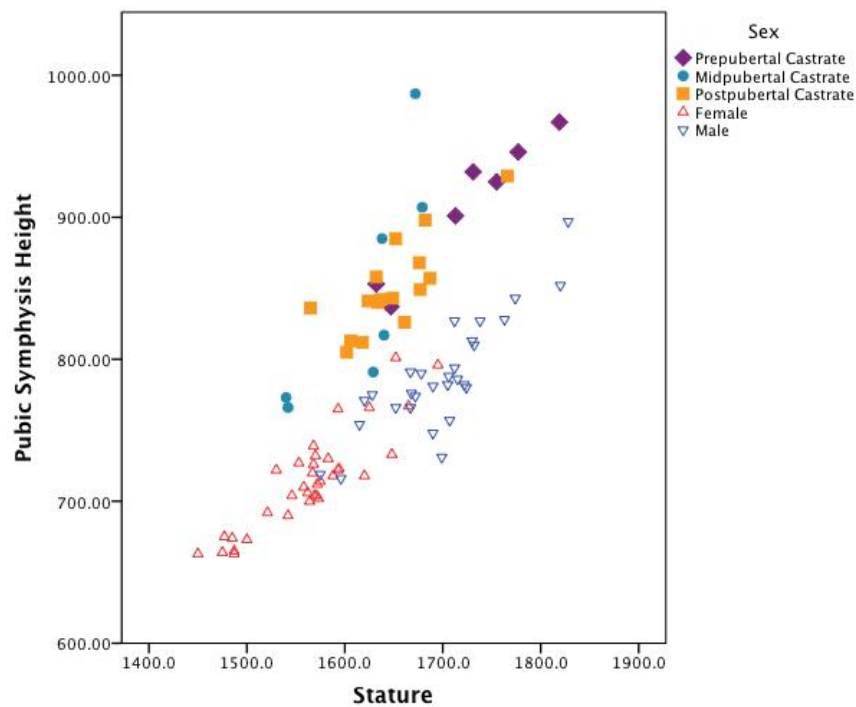


Figure 6.29: Comparison of stature to pubic symphysis height (in mm) in the Asian population, showing the clear separation of the castrates from the males and females (castrate data from Wagenseil, 1933).

Comparison of Pubic Symphysis Height and Stature in All Populations

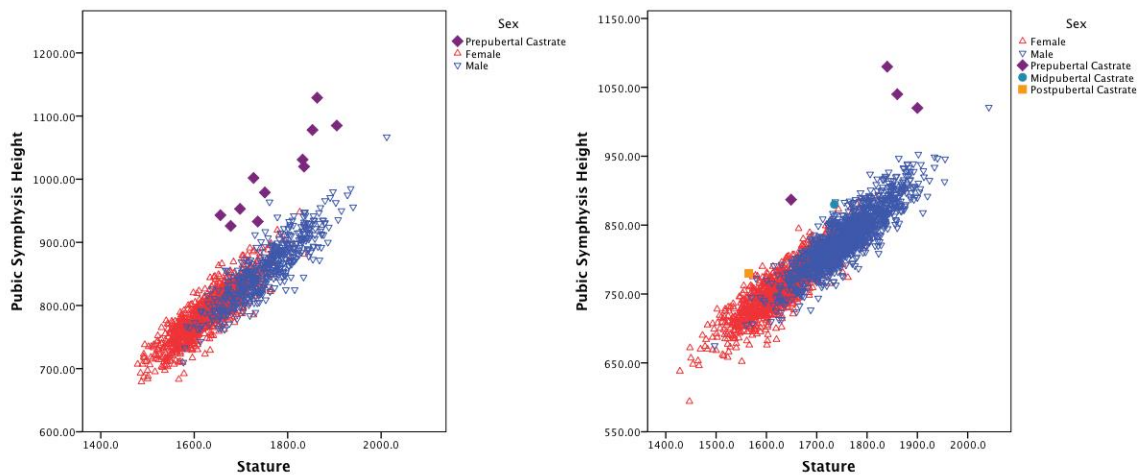


Figure 6.30: Comparison of stature to pubic symphysis height (in mm) in the African (left) and European (right) populations, showing the separation between the castrates and the males and females, with those Europeans castrated postpubertally falling closer to the normal population, as expected (castrate data from Koch, 1921 and Wagenseil, 1927).

6.2.2 Animals

6.2.2.1 Metric Analysis

There are almost no studies of the effects of castration on living animals similar to the anthropometric studies undertaken on living human castrates. Some veterinarians or agricultural specialists mention observations on steer hindquarters,⁵¹² but few published studies exist. Although it would be reasonable to think that chimpanzees, due to the similarity in genetic make-up, could be used as proxies for humans, studies by Clark and Gavan suggest otherwise.⁵¹³

The second of the two studies is a small sequel to a paper about the effects of castration in the chimpanzee and compared data from the deceased subject of the original paper and a second prepubertally castrated chimpanzee to data taken from thirteen non-castrated male chimpanzees being kept for a growth study.⁵¹⁴ Of the fifteen apes studied, six (five of them non-castrated and the castrated chimpanzee from the original paper) had been used for other studies involving sex administration of exogenous hormones. The authors stated that they castrated the second chimpanzee and published the 1962 paper because the first castrated chimpanzee had not shown signs of the extensive long bone growth resulting from open epiphyses that had been reported in human castrates.

⁵¹² (Flood, 1899; Luff, 1994)

⁵¹³ (1962)

⁵¹⁴ (Clark and Gavan, 1962)

Comparison of Total Leg Length and Sitting Height in the Total Chimpanzee Population

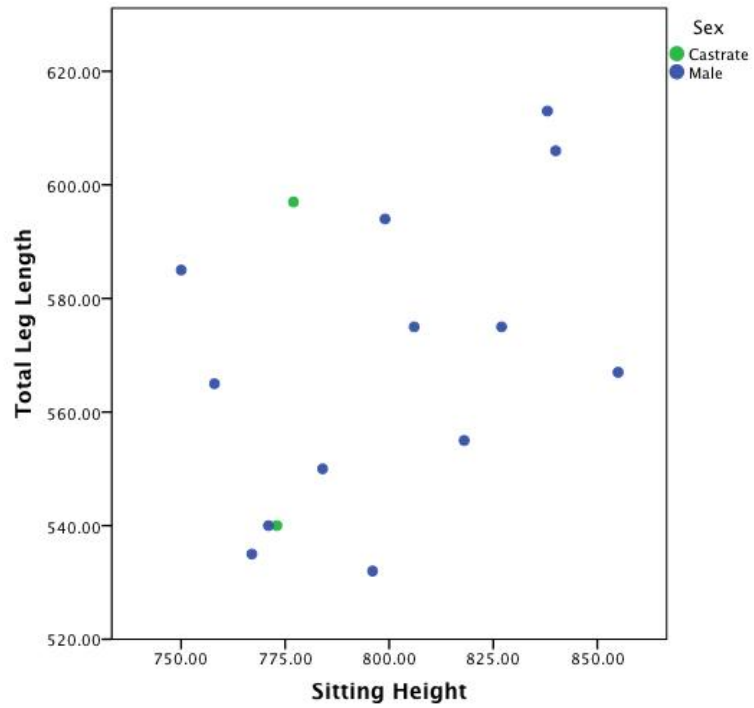


Figure 6.31: Comparison of chimpanzee sitting height to total leg length (in mm) as shown in Clark and Gavan (1962).

Comparison of Total Leg Length and Sitting Height in the Non-Hormonally Altered Chimpanzee Population

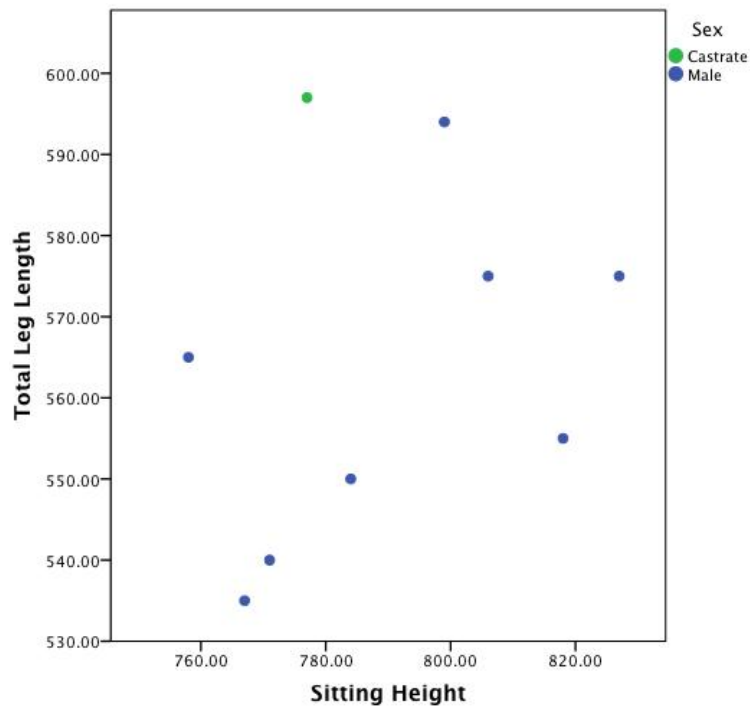


Figure 6.32: Comparison of the sitting height to the total leg length (in mm) of the prepubertally castrated chimpanzee against the non-castrated chimpanzees from the non-hormonally altered group (graph produced by author from data from Clark and Gavan, 1962).

Radiographs of the long bones of both prepubertal castrates showed open epiphyses beyond the age at which the epiphyses of a non-castrated male had already fused. Clark and Gavan stated that although the castrated chimpanzees had open epiphyses for a few extra years, there was no “marked” excess growth of the long bones as had been seen in humans. However, they took no direct long bone measurements and had plotted only the sitting height (i.e., torso length) of the chimpanzees against a summed leg length acquired from adding the tibial and thigh lengths (**Figure 6.31**). As no overall stature was given for the chimpanzees, it is impossible to judge the thigh, tibia, torso, and leg sum measurements against the stature, which would more closely approximate the human studies discussed in the previous section. When the six chimpanzees that had been used in hormonal experiments were removed from the population, the remaining prepubertally castrated chimpanzee is somewhat distinguished from the remaining non-castrated chimpanzees, mostly by the summed length of his legs (**Figure 6.32**). The crural index (tibial length x 100/femoral length) differentiates the castrated chimpanzee slightly better, with the non-hormonally altered group of chimpanzees displaying a much smaller variation in the ratio that is distinct from the ratio of the castrated chimpanzee (**Figure 6.33**).

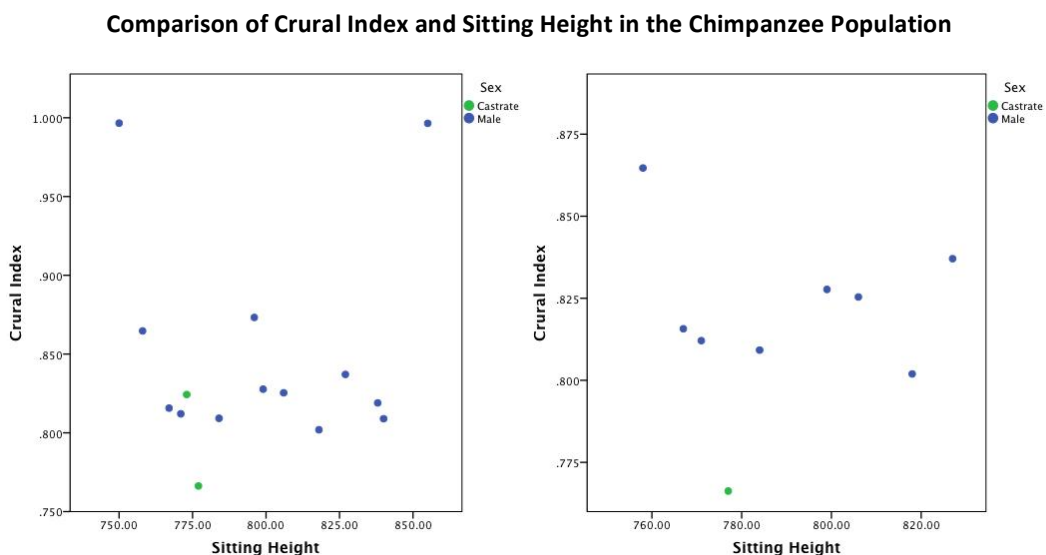


Figure 6.33: Crural index versus sitting height (in mm) showing the total chimpanzee population (left) and the non-hormonally altered chimpanzee population (right) (left as in Clark and Gavan, 1962, right produced by author from data from the paper).

In the non-hormonally altered group of chimpanzees, if the relationship between the lengths of the tibia and thigh (i.e., the femur) is examined (**Figure 6.34**), it is easy to

see that the castrated chimpanzee is well separated from the non-castrated males by the length of his thigh. Similarly, when the length of the thigh is compared to the sitting height (**Figure 6.35**), the castrated chimpanzee stands out from the non-castrated males, again due to the length of his thigh. However, when the length of the tibia is compared to the sitting height (**Figure 6.36**), the castrated chimpanzee falls within the upper ranges of male length, not differentiated from the non-castrated males at all. Thus, it seems that castration is more strongly affecting the proximal portion of the legs in the chimpanzee, rather than the distal portion of the legs, as seen in humans. Additionally, while the macroscopic examination of the skeletons of the castrated chimpanzees did not appear to display exaggerated long bone growth, it is still possible to differentiate between the castrated and non-castrated chimpanzees through careful analysis of their measurements.

Comparison of Thigh Length and Tibia Length in the Non-Hormonally Altered Chimpanzee Population

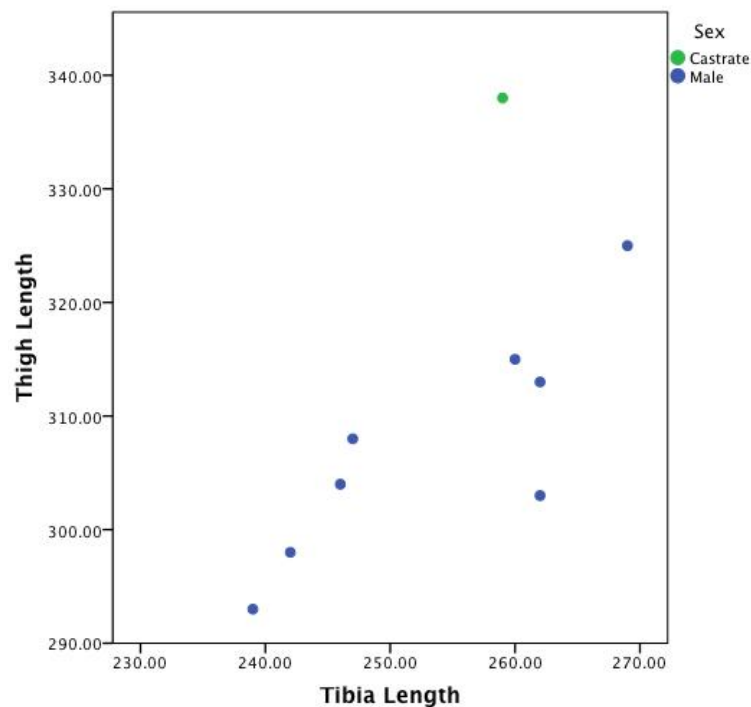


Figure 6.34: Comparison of castrate to non-castrate tibia length to thigh length (in mm) in the series of non-hormonally altered chimpanzees (graph produced by author from data from Clark and Gavan, 1962).

Comparison of Thigh Length and Sitting Height in the Non-Hormonally Altered Chimpanzee Population

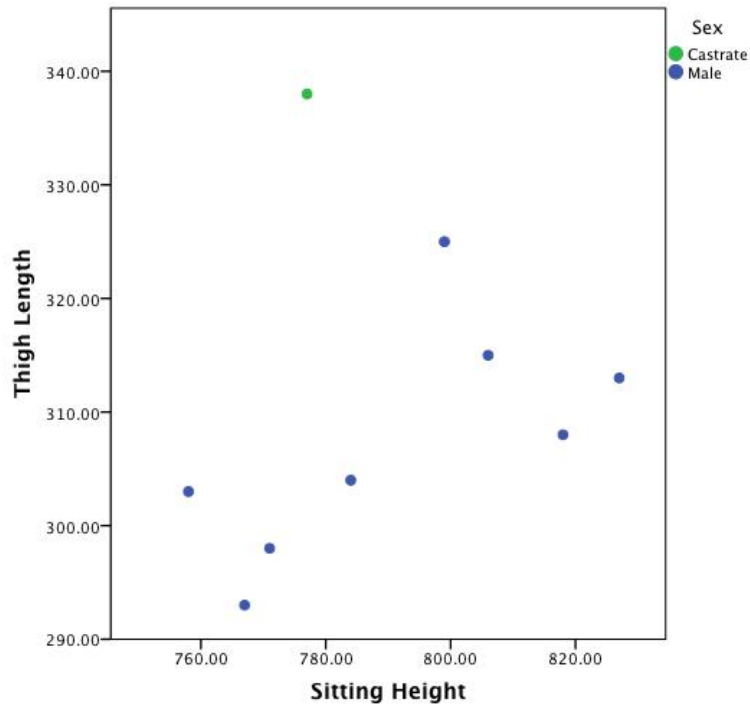


Figure 6.35: Comparison of castrate versus non-castrate sitting height to thigh length (in mm) in the non-hormonally altered group of chimpanzees (graph produced by author from data from Clark and Gavan, 1962).

Comparison of Tibia Length and Sitting Height in the Non-Hormonally Altered Chimpanzee Population

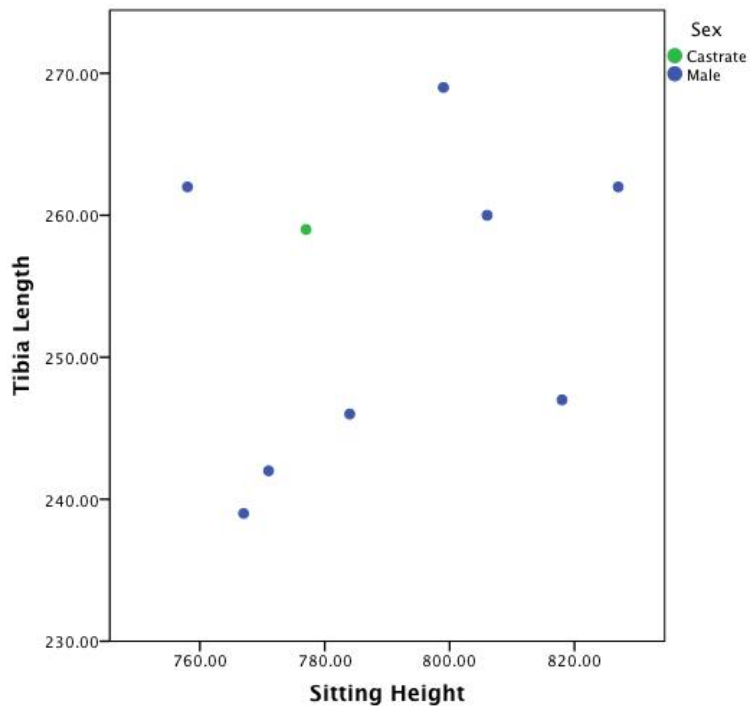


Figure 6.36: Comparison of castrate versus non-castrate sitting height to tibia length (in mm) in the non-hormonally altered group of chimpanzees (graph produced by author from data from Clark and Gavan, 1962).

6.3 Results of Statistical Analysis

6.3.1 Humans

6.3.1.1 Anthropometric

Statistical analysis of the anthropometric data was run using linear discriminant function analysis (LDA) and Mahalanobis distance discriminant function analysis (MDDFA). Both methods showed good separation between the castrates and the intact males and females. As Tandler and Grosz did not give as many measurements in their examination of the Skoptsy as Wagenseil gave in his examinations of the Turkish and Chinese castrates, it was not possible to include them in the linear discriminant function analysis, as they did not have sufficient variables.

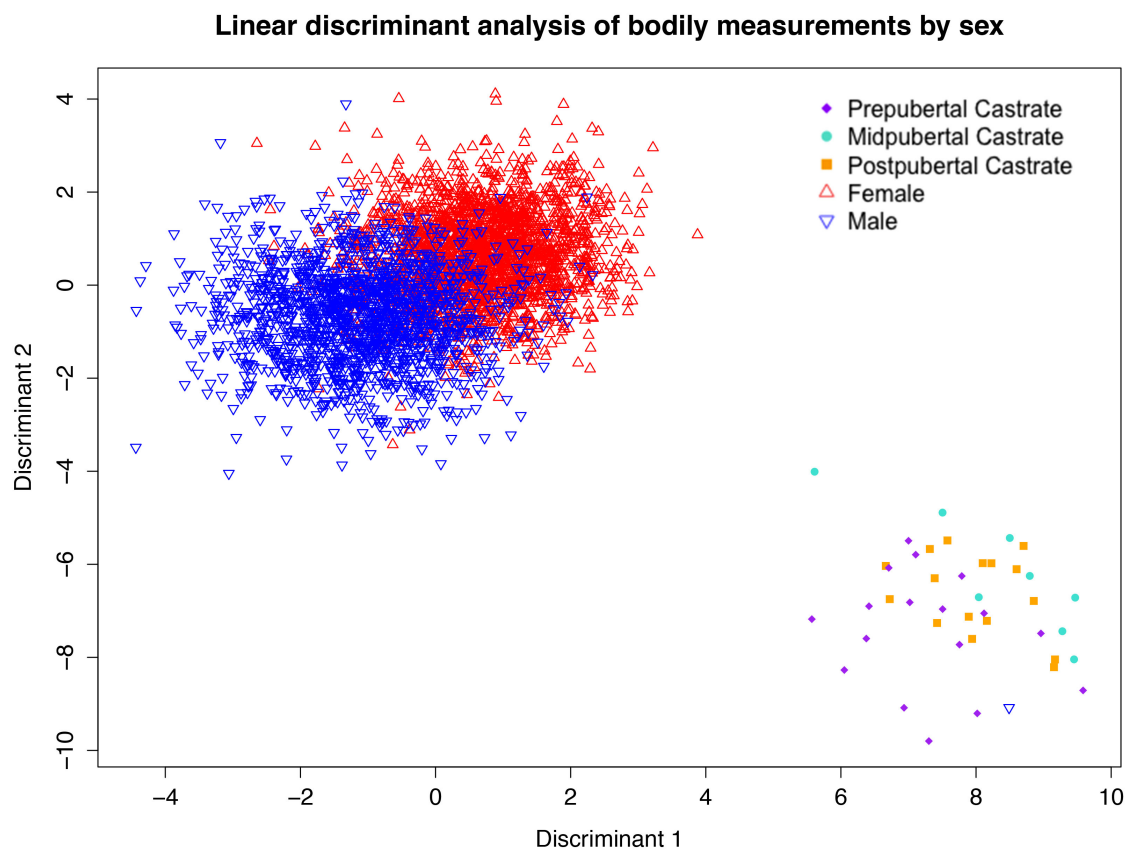


Figure 6.37: Result of the anthropometric linear discriminant function analysis using sex as the grouping variable and showing the distribution of sexes and age of castration, showing the clear separation of the castrates from the males and females. The single male grouped with the castrates is the Wagenseil African comparison. (Castrate data from Tandler and Grosz, 1910; Wagenseil, 1933, 1927, graph by author)

The analysis of the anthropometric dataset was begun by running an LDA using only a single categorical variable such as sex (Castrate, Female, and Male), ancestry (Caucasoid, Negroid, or Mongoloid), or sex taking into account age of castration (Prepubertal Castrate, Midpubertal Castrate, Postpubertal Castrate, Female, and Male) in

the analysis and as the grouping variable. Using the three sex categories meant that only two functions would be generated to account for all variation. The first function achieves a separation among the three classes of 60.85%, and the second function accounts for the remaining 39.15% of the variation. This means that a good amount of separation is achieved by the first function, but the second function should also be used to achieve the best separation of the groups, as it also accounts for a large proportion of the variation. These results were statistically significant, with the first function ($df = 8, p < 0.0005, \text{Wilk's } \Lambda = 0.209$) contributing more to the separation of the groups than the second ($df = 3, p < 0.0005, \text{Wilk's } \Lambda = 0.515$). In contrast, using the five sex and age categories

Linear discriminant analysis of bodily measurements by ancestry

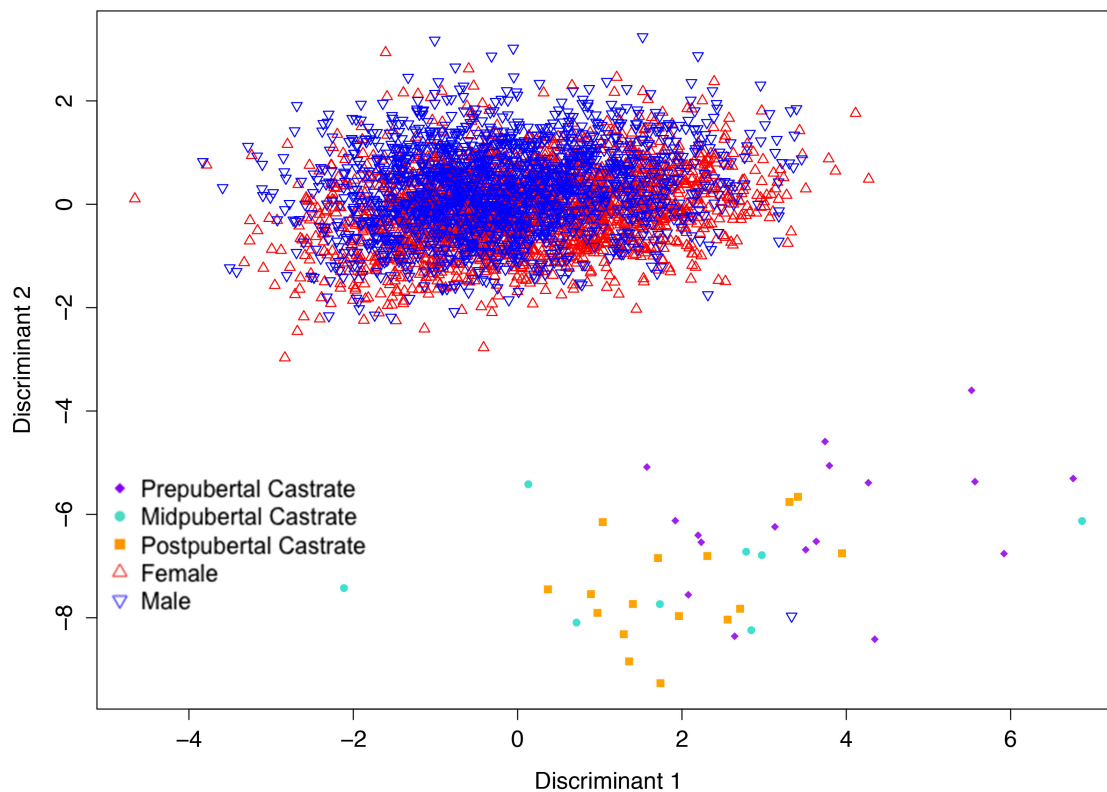


Figure 6.38: Graph displaying the results of the linear discriminant function analysis using ancestry as the grouping variable and showing the distribution of sexes and age of castration, showing a clear separation between the males and females and the castrates, but with considerable overlap in the males and females. The single male grouped with the castrates is the Wagenseil African comparison. (Castrate data from Tandler and Grosz, 1910; Wagenseil, 1933, 1927, graph by author)

generated four functions to account for all variation, with 60.34% accounted for in the first function ($df = 16, p < 0.0005, \text{Wilk's } \Lambda = 0.204$), 38.92% in the second function ($df = 9, p < 0.0005, \text{Wilk's } \Lambda = 0.504$), 0.72% in the third function ($df = 4, p < 0.0005, \text{Wilk's } \Lambda = 0.982$), and 0.01% in the final function ($df = 1, p = 0.242, \text{Wilk's } \Lambda = 1.0$).

This suggests that the age of castration does not strongly affect the variation between males, females, and castrates, as the additional age categories for the castrates do not generate extra functions that account for large amounts of variation in the groups. When grouping by ancestry but accounting for the age of castration, 79.5% separation was achieved in the first function ($df = 12$, $p < 0.0005$, Wilk's $\Lambda = 0.454$), and 20.5% of all variation was accounted for in the second ($df = 5$, $p < 0.0005$, Wilk's $\Lambda = 0.826$).

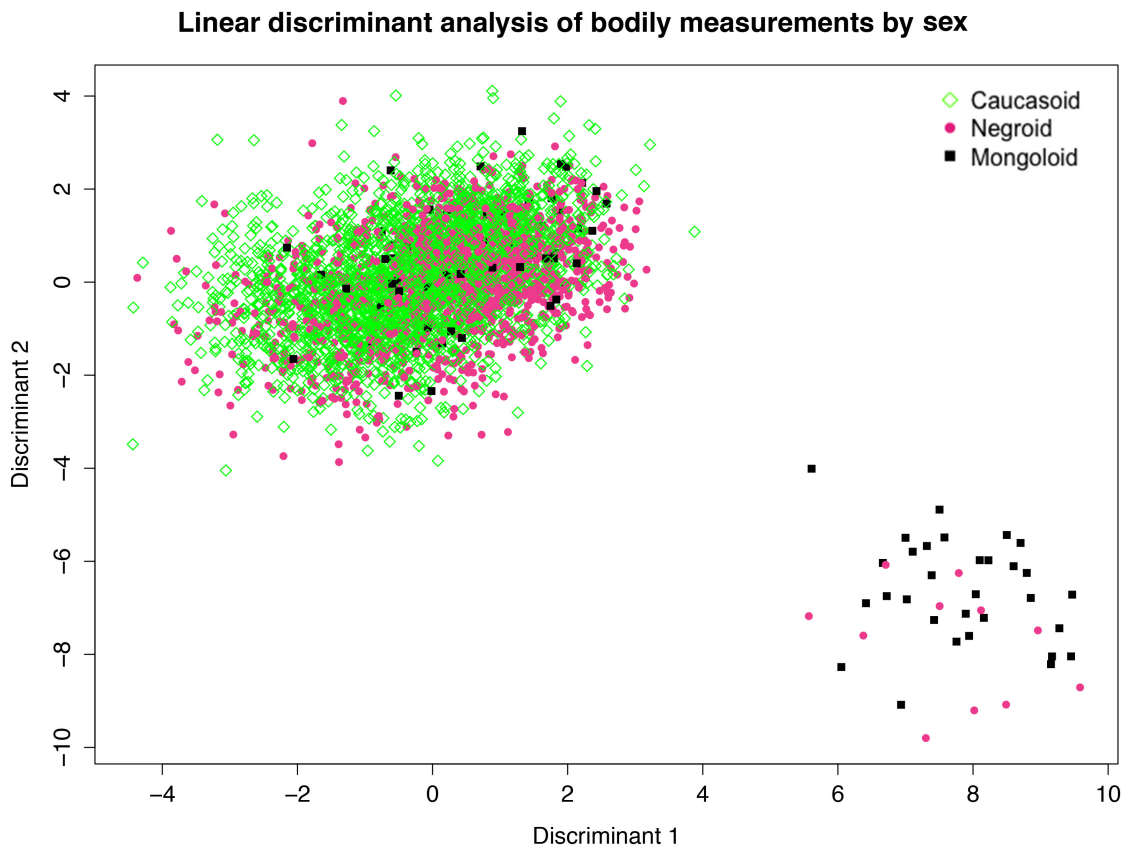


Figure 6.39: Result of the anthropometric linear discriminant function analysis using sex as the grouping variable but showing the distribution of ancestry, showing the clear separation of the castrates from the males and females. The single male grouped with the castrates is the Wagenseil African comparison. (Castrate data from Tandler and Grosz, 1910; Wagenseil, 1933, 1927, graph by author)

Once the analyses using single variables were completed, analyses were run using sex, ancestry, and age of castration as variables in the same analysis, grouping by sex and then by ancestry. Whether grouping by sex or ancestry, the results for sex and age of castration did not vary, and their graphical results show clear separation between the males and females and the castrates (**Figures 6.37 & 6.38**).

The results of the analyses appear to indicate that the majority of variation is due to sex, rather than ancestry, as can be seen in all of the graphs (**Figures 6.37 – 6.40**). Note that no matter the ancestry, the castrates still separate from the male and female

groups. Ancestry does play a part in differentiating the groups (as seen in **Figures 6.39 & 6.40**), but it is clearly sex that is the most important variable in separating the castrates, males, and females.

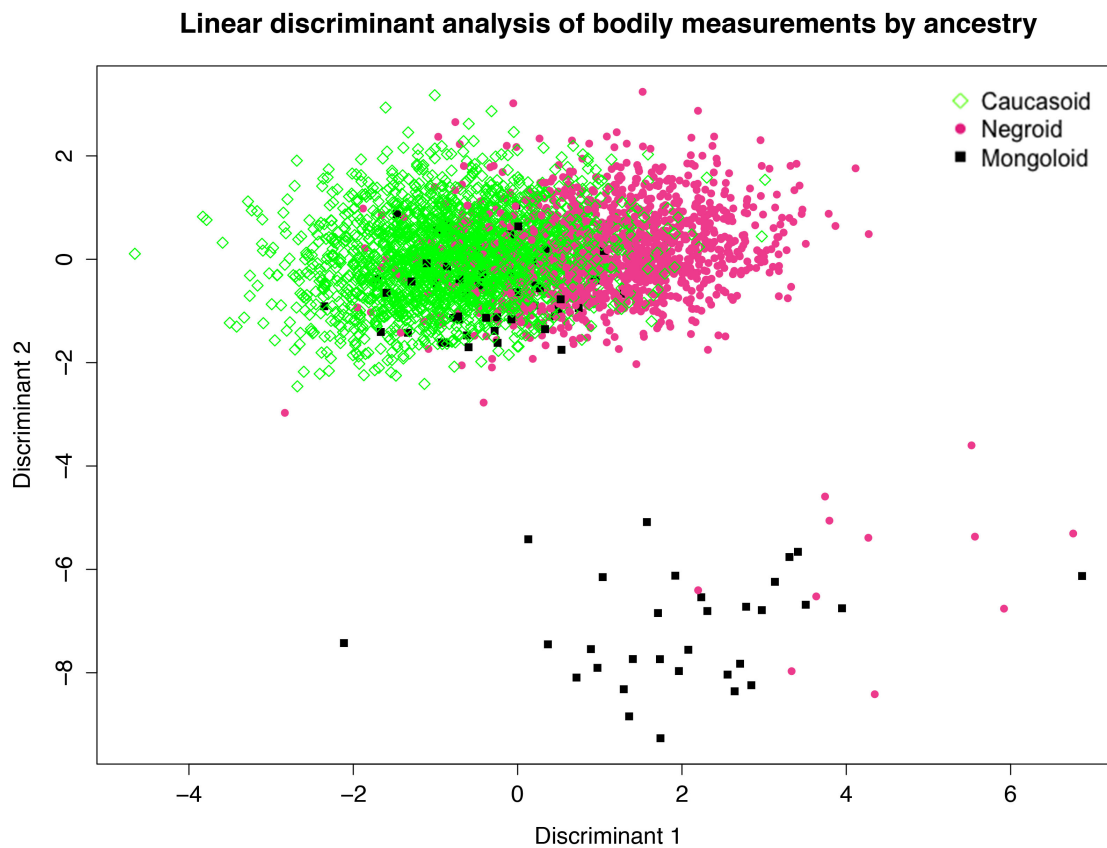


Figure 6.40: Graph displaying the results of the linear discriminant function analysis using ancestry as the grouping variable and showing the distribution of ancestry, showing a clear separation between the males and females and the castrates, but with considerable overlap in the males and females. The single male grouped with the castrates is the Wagenseil African comparison. (Castrate data from Tandler and Grosz, 1910; Wagenseil, 1933, 1927, graph by author)

The results of the anthropometric Mahalanobis distance discriminant function analysis for the first fifty individuals in the dataset are summarized in **Table 6.1**. In the table, for each individual, the smallest number (the Mahalanobis distance) of the three subheadings (Castrate, Female and Male) designates the group to which the individual is assigned, no matter what the original assignment (Sex) was. For example, individual number one, a castrate, received the lowest of the three scores for the Castrate category. Therefore, this individual was correctly assigned to the castrate group. As can be seen, all the castrates received the smallest scores in the Castrate column. However, individual number forty-five, the Sudanese “normal”, reportedly non-castrated male that Wagenseil

used as a control for his African “Turkish” castrates,⁵¹⁵ has also been assigned to the castrate group. This individual has been consistently closer to the castrate group in all of the above LDA, raising doubts as to his status as an intact male. Alternatively, as East African individuals are recognized as being long-legged in comparison to Europeans, Asians, or even other Africans, perhaps this characteristic figures into this anomaly. In addition, numbers seventy-three and seventy-six, both females, would be assigned to the male group based upon their scores. These results may reflect the overlap between males and females already seen in **Figures 6.16-6.20**. Overall, the correct classification for individuals in the anthropometric dataset using Mahalanobis distance was 87.0%. The results shown in this table (**Table 6.1**) indicate that Mahalanobis distance discriminant function analysis is a good method of separating castrates from males and females but may not be as effective at separating groups when a large overlap (such as that between the males and females) is known to exist.

Results of the Anthropometric Mahalanobis Distance Discriminant Function Analysis

Individual	Sex	Castrate	Female	Male	Individual	Sex	Castrate	Female	Male
1	1	35.0614454	92.871888	97.989013	26	1	4.9474795	53.176383	57.76963
2	1	5.3857966	48.184898	50.725979	27	1	2.3316888	57.271529	61.333599
3	1	3.1218776	64.82799	62.973311	28	1	0.3109057	44.932424	46.284094
4	1	2.8314442	47.68635	53.166209	29	1	9.6765575	24.545619	27.588268
5	1	8.4923599	50.967807	56.310874	30	1	5.5541534	57.637302	59.808836
6	1	5.4226102	59.726878	62.170778	31	1	1.6460065	38.132451	40.045465
7	1	8.5983636	42.768034	45.942973	33	1	24.0864004	62.982592	61.851755
8	1	0.992279	42.783894	43.14403	34	1	10.1624408	56.992201	56.430307
9	1	10.9830101	66.959427	68.093232	35	1	3.9422264	77.894715	80.462857
10	1	1.9240049	69.957652	73.225258	36	1	14.1369408	83.344943	81.151828
11	1	8.4772715	76.215183	78.75151	37	1	6.3147642	67.125931	70.485892
12	1	2.4163669	39.60804	42.471701	38	1	33.3040114	101.875534	101.620888
13	1	4.3687698	48.716805	52.75125	39	1	9.7798123	46.732538	48.720933
14	1	9.6689626	42.191606	46.825919	40	1	1.5050455	49.990446	51.887258
15	1	6.5539667	56.269181	59.208432	41	1	12.7424432	65.310942	68.067755
16	1	3.0578458	45.419747	46.44273	42	1	6.4067832	50.926924	54.256352
17	1	14.323922	76.516483	80.453766	45	3	2.7673492	73.313128	73.772315
18	1	1.4091642	38.80051	42.170634	70	2	66.1569413	2.755514	2.91066
19	1	5.9742179	62.059289	63.642106	71	2	66.9135938	3.85874	8.588388
20	1	4.3362845	54.688423	52.63733	72	2	56.5466067	3.13715	5.914453
21	1	4.1745425	54.617487	55.913253	73	2	38.2223004	7.171599	3.125856
22	1	3.5039585	41.061326	45.002725	74	2	66.1383381	2.485995	6.305003
23	1	1.1152382	51.461354	56.220638	75	2	55.7393767	1.483298	6.991971
24	1	4.6942809	71.195471	74.002616	76	2	51.7375893	10.617557	5.376403
25	1	0.6012449	45.627525	49.896201	77	2	63.2575969	1.229434	3.11762

Table 6.1: First fifty results of the anthropometric Mahalanobis distance discriminant function analysis grouping by sex and using sex, ancestry, age of castration, stature, arm length, height of the anterior superior iliac spine, and pubic symphysis height as variables. For the sex column, 1 = Castrate, 2 = Female, and 3 = Male. (Castrate data from Tandler and Grosz, 1910; Wagenseil, 1933, 1927, table by author)

⁵¹⁵ (Wagenseil, 1927)

6.3.1.2 Conversion of Anthropometric to Osteometric Measurements

In an effort to establish the best way to combine osteometric and anthropometric measurements, cadavers at the Medical Sciences Training Centre at the Department of Physiology, Anatomy, and Genetics, University of Oxford, were examined. In order to determine the relationship between tarsal height and pubic symphysis height, a number of measurements corresponding to skeletal landmarks were taken. It was found that the height of the medial malleolus was on average eleven centimetres of the total pubic symphysis height and that the measurement ranged from eight to thirteen centimetres.

In his article on Turkish castrates,⁵¹⁶ Wagenseil lists a large number of measurements taken using Martin's anthropometric standards,⁵¹⁷ as described in Chapter Three. Twelve of these measurements are taken from skeletal landmarks and either directly correspond to or can be calculated to gain osteometric measurements (**Figure 6.41**), which allows the anthropometric data to be converted to osteometric data. This provides measurements for the approximate lengths of the humerus, radius, femur, and tibia, allowing anthropometric measurements to be converted to osteometric measurements. As Wagenseil only supplied a detailed set of measurements for the Turkish castrates,⁵¹⁸ and the ANSUR data were taken on the lateral rather than medial aspects of the legs, the African-born Turkish castrates were the only individuals it was possible to add to the osteometric dataset for statistical analysis.

⁵¹⁶ (Wagenseil, 1927)

⁵¹⁷ (Martin, 1914)

⁵¹⁸ (Wagenseil, 1927)

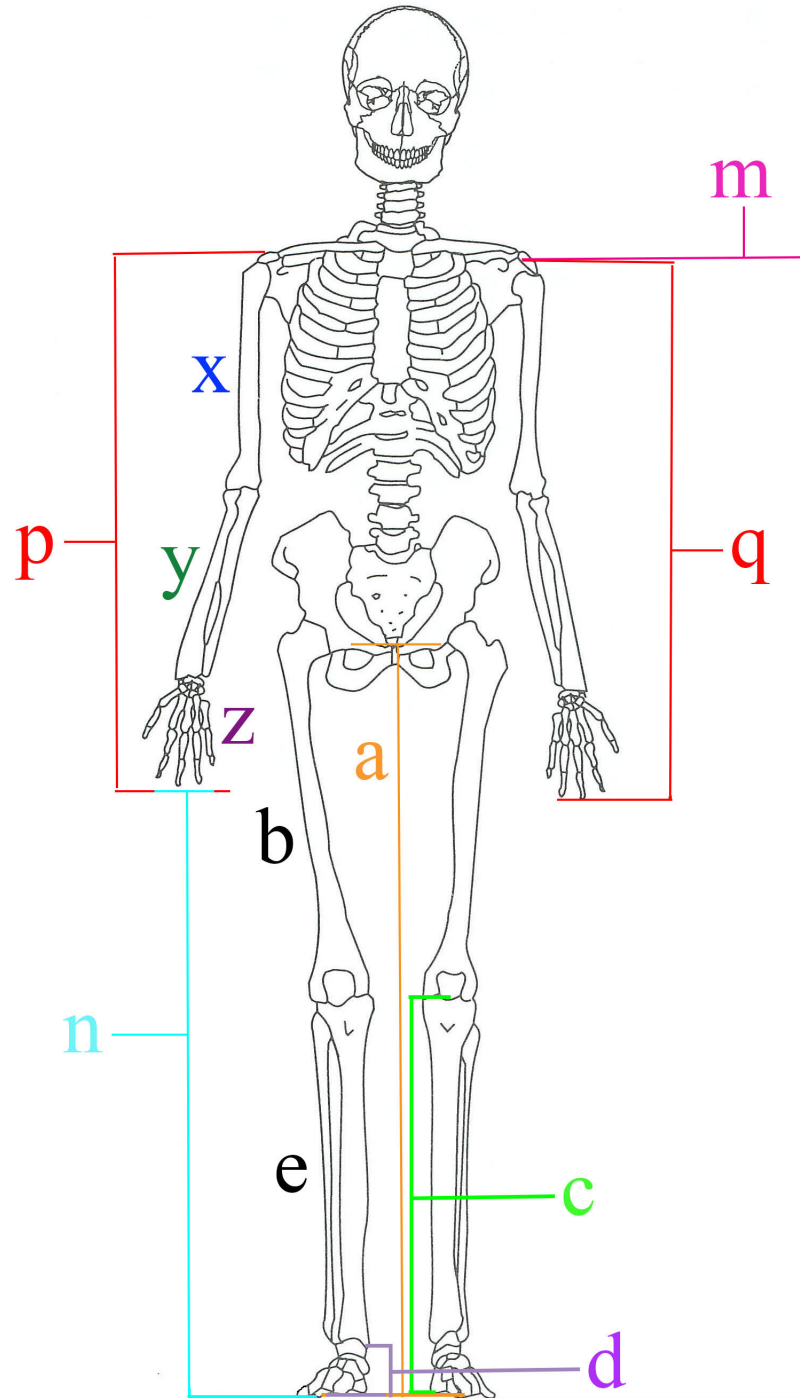


Figure 6.41: Diagram of anthropometric measurements given in Wagenseil (1927) and the osteometric equivalents. Measurement a is the height of the pubic symphysis from the floor, c is the height of the joint of the knee (the upper edge of the medial tibial epicondyle) to the floor, d is the height of the medial malleolus to the floor, m is the height of the shoulder (top of the acromion) from the floor, n is the height of the tip of the middle finger from the floor, x is the length of the upper arm, y is the length of the lower arm, z is the length of the hand, p is the sum of x, y, and z, and q is the difference between m and n. Measurements b and e must be calculated. Measurement b can be calculated by subtracting c from a, and measurement e can be calculated by subtracting d from c. (Skeleton from Buikstra and Ubelaker, 1994, lines and colouring by author.)

6.3.1.3 Osteometric

There were not sufficient measurements from known castrate skeletal remains to run linear discriminant function analysis on only the osteometric material. Using Wagenseil's Turkish anthropometric measurements converted to osteometric measurements (as discussed above), a calibrated dataset was created in order to run osteometric linear discriminant function analyses. As Wagenseil's measurements were taken on the right side of the body, only right side skeletal elements were included in the osteometric dataset, limiting the number of individuals in the dataset to just over three hundred. All of the Turkish castrates were prepubertally castrated, and only two of the castrates in the original osteometric dataset were postpubertal, so the age of castration was not considered in these analyses.

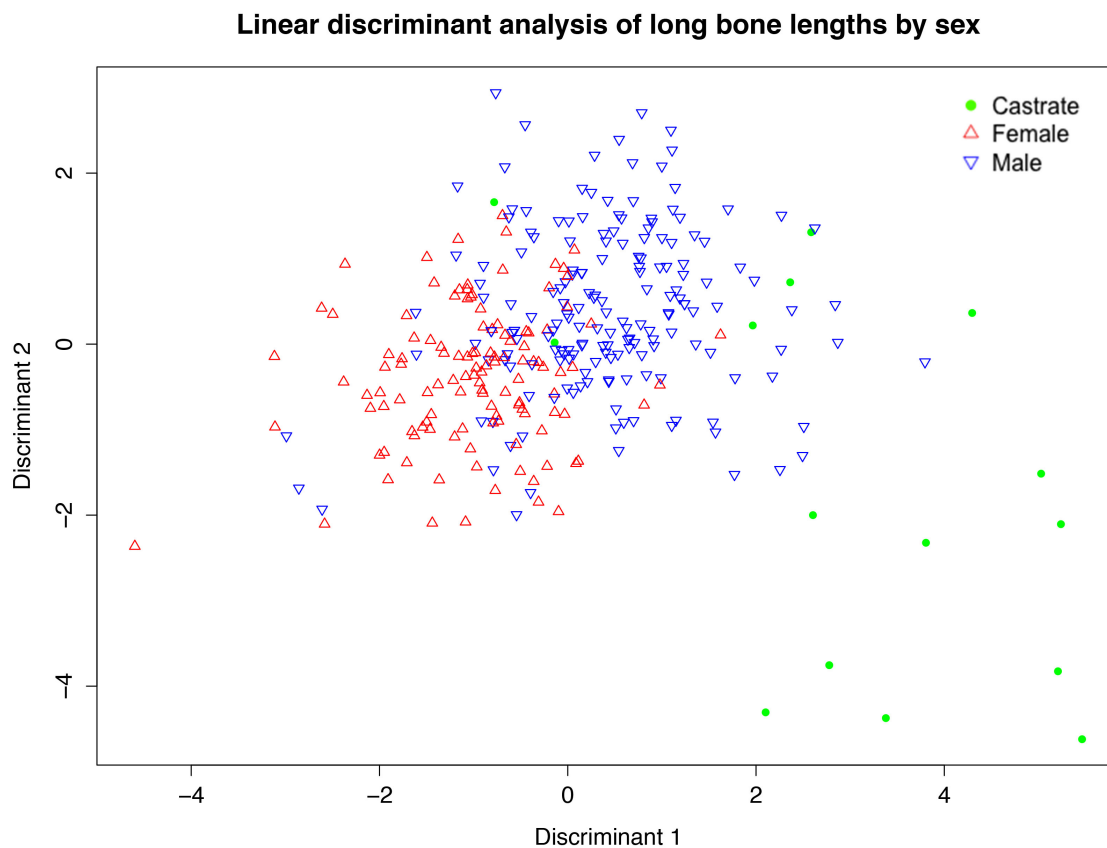


Figure 6.42: Graphical result of the osteometric linear discriminant function analysis using sex as the grouping variable and showing the distribution of sex. There is not such a clear separation of the castrates from the males and females in the osteometric dataset as there was in the anthropometric dataset. (Castrate data from Eng et al., 2010; Wagenseil, 1927, and author, graph by author)

Linear discriminant analysis of long bone lengths by sex

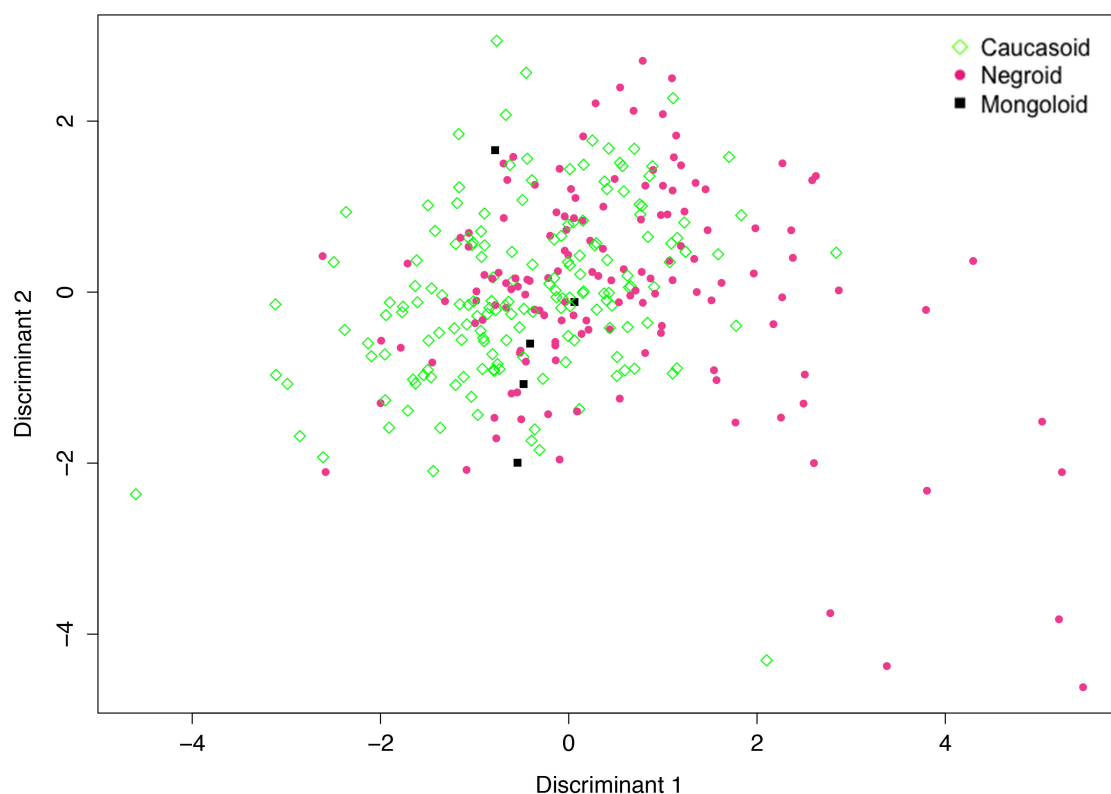


Figure 6.43: Graphical result of the osteometric linear discriminant function analysis using sex as the grouping variable and showing the distribution of ancestry. There is not such a clear separation of the castrates from the males and females in the osteometric dataset as there was in the anthropometric dataset. (Castrate data from Eng et al., 2010; Wagenseil, 1927, and author, graph by author)

The linear discriminant function analyses of the osteometric dataset revealed an unexpected finding: the analysis gave much better results using ancestry as a grouping variable than it did for sex. As above, both sex and ancestry had only two functions to account for all variation within the dataset, but sex only accounted for 77.39% of the variation in the first function ($df = 8$, $p < 0.0005$, Wilk's $\Lambda = 0.406$) and 22.61% of the variation in the second function ($df = 3$, $p < 0.0005$, Wilk's $\Lambda = 0.785$). In contrast, ancestry accounted for 98.26% of all variation in the first function ($df = 8$, $p < 0.0005$, Wilk's $\Lambda = 0.786$), with only 1.74% of variation accounted for by the second function ($df = 3$, $p < 0.0005$, Wilk's $\Lambda = 0.995$), indicating that the three groups could be almost entirely separated using only the first function. There appears to be better separation by ancestry in the osteometric dataset, though this may be because the majority of the castrates within the dataset are Wagenseil's African castrates. This is shown in the graphs of the discriminant functions (**Figures 6.42 – 6.45**), with considerable overlap among the three sexes in the graphs of the analyses grouped by sex (**Figures 6.42 &**

6.43) and less but still noticeable overlap among the sexes in the graphs of the analyses grouped by ancestry (Figures 6.44 & 6.45).

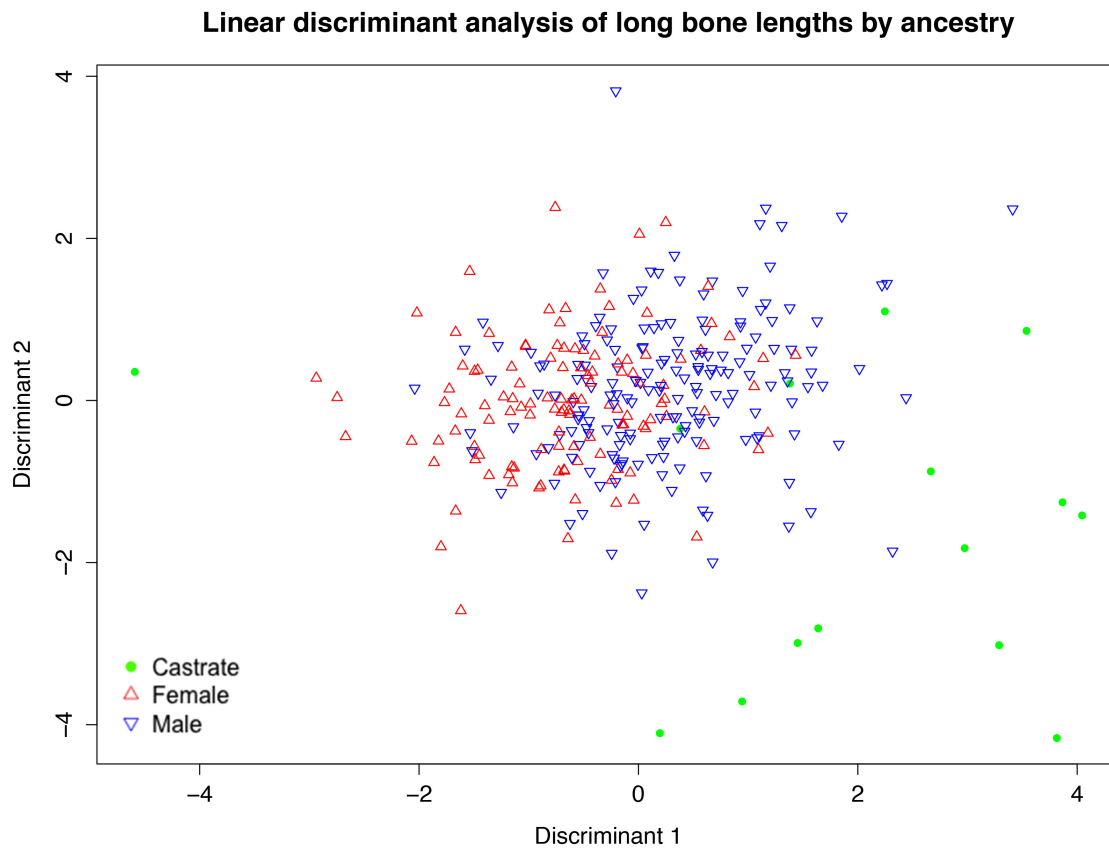


Figure 6.44: Graphical result of the osteometric linear discriminant function analysis using ancestry as the grouping variable and showing the distribution of sex. There is not such a clear separation of the castrates from the males and females in the osteometric dataset as there was in the anthropometric dataset. (Castrate data from Eng et al., 2010; Wagenseil, 1927, and author, graph by author)

Linear discriminant analysis of long bone lengths by ancestry

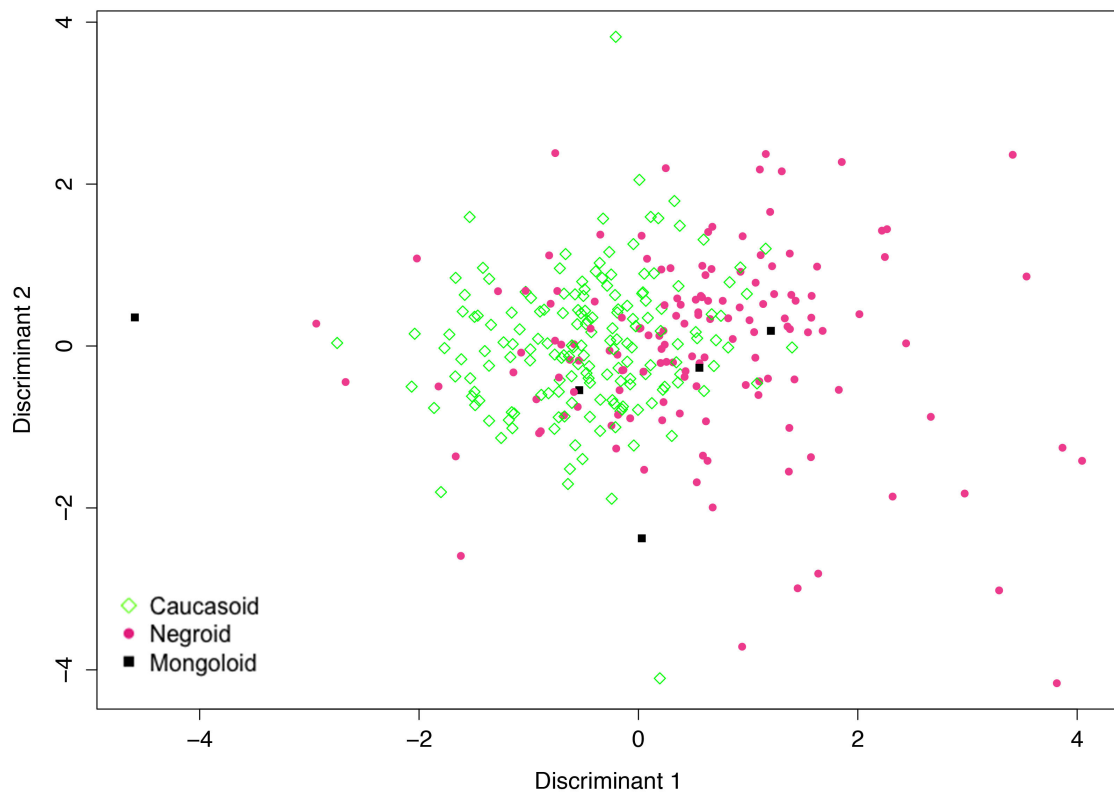


Figure 6.45: Graphical result of the osteometric linear discriminant function analysis using ancestry as the grouping variable and showing the distribution of ancestry. There is not such a clear separation of the castrates from the males and females in the osteometric dataset as there was in the anthropometric dataset. (Castrate data from Eng et al., 2010; Wagenseil, 1927, and author, graph by author)

The results of the Mahalanobis distance discriminant function analysis of the osteometric data are somewhat mixed (**Table 6.2**). Of the fifteen castrates within this dataset, five are misclassified, and of the remaining thirty-five non-castrated individuals in the table, nine are misclassified, leading to a total of fourteen misclassifications out of fifty individuals, for a misclassification rate of 28%. The total dataset gave an 82.2% correct classification rate.

If it were possible to get more castrate and intact human skeletal data, it is possible that these analyses would yield better results. The anthropometric dataset had over three thousand individuals, while the osteometric dataset had only just over three hundred. If more skeletal data were obtained, especially data that had a closer geographic and temporal relationship to the castrate skeletons included here, this type of analysis might better separate the castrates from the intact humans, leading to improvement in statistical determinations of castrate status within osteological populations.

Results of the Osteometric Mahalanobis Distance Discriminant Function Analysis

Individual	Sex	MD.castrate	MD.female	MD.male	Individual	Sex	MD.castrate	MD.female	MD.male
1	1	8.5790482	10.5370276	4.7198088	28	3	2.6635147	6.8112996	5.652981
2	1	3.8456457	5.351053	1.7778936	29	3	6.3523833	4.7845171	1.3138508
4	1	53.3973446	40.446061	39.1508318	30	3	20.4684079	11.66171	7.5184367
5	1	8.859271	1.8789351	1.643784	32	2	10.9351533	3.6929967	2.7526341
6	1	3.5245786	21.3983382	15.4386871	33	2	12.8331927	5.5976476	5.8967503
7	1	6.4251382	29.6445811	26.2445375	37	3	12.6209501	2.1097737	3.1237397
8	1	3.5988599	12.2080411	10.4041059	40	3	7.7493313	4.96246	3.5407526
9	1	4.8451258	24.7803896	19.2326302	41	3	8.4088987	1.8441689	3.7691029
10	1	12.0725013	14.252797	9.4784654	45	3	8.2310479	0.9035178	0.3568477
11	1	8.9162746	19.9660398	12.788029	57	3	7.6429639	2.8347058	2.8144885
12	1	11.440089	37.3184867	34.5122428	59	3	6.8459249	5.4485803	4.0585611
13	1	3.6738865	16.499745	16.5844137	60	3	6.76849	1.8625808	1.575793
14	1	1.5793088	15.8956448	12.7216557	65	2	9.6047667	1.935227	3.6989356
15	1	8.0181549	24.6100364	24.5664615	67	2	12.0863838	2.1826906	3.5366082
17	1	9.2275988	20.2967095	22.0490822	73	3	12.0389421	5.005741	2.5196317
18	3	0.4962591	6.5696342	4.6303772	74	3	5.9425099	2.1752188	0.7495326
19	3	11.1242056	2.7098116	3.503151	76	2	13.9055124	3.260738	5.1486901
20	3	5.2448671	8.8075029	5.6520352	79	3	8.3026922	1.5884817	0.4789141
21	2	7.2694799	1.4686744	1.9727808	83	3	11.5888105	4.697127	5.6185858
22	3	9.2501254	2.6600898	1.1739248	84	3	11.6698706	6.2351599	2.8992405
23	2	8.6734128	1.0686231	0.7711856	91	2	15.5421889	1.5282907	4.2944137
24	3	14.4640159	5.1376572	2.2705995	95	2	26.2073502	6.9898823	11.3291839
25	3	6.1642899	4.6639762	1.8130876	98	3	11.005687	4.2207694	4.0675432
26	2	9.4524126	1.2061231	1.502944	99	3	7.2837731	1.4155205	1.0497821
27	3	13.9430694	9.3398816	5.9313611	104	2	9.3038307	1.0170119	3.6153131

Table 6.2: First fifty results of the osteometric Mahalanobis distance discriminant function analysis grouping by sex and using sex, ancestry, humeral length, radial length, femoral length, and tibial length as variables. (Castrate data from Eng et al., 2010; Wagenseil, 1927, and author, table by author)

6.3.2 Animals

6.3.2.1 Osteometric

The linear discriminant function analysis of the Davis sheep data showed good results for osteological material in contrast to the human osteological material discussed above. The analysis was originally run on the total dataset, using all the available length, breadth, and circumference variables. The analysis produced the two functions to account for all variation within the variables, with the first function accounting for 74.87% of the variation ($df = 40$, $p < 0.0005$, Wilk's $\Lambda = 0.039$) and the second function for 25.13% of the variation ($df = 19$, $p < 0.0005$, Wilk's $\Lambda = 0.305$). The graphical results are displayed in **Figure 6.46**. As can be seen, there is clear separation of the three groups, with only a very small overlap between the males and the castrates, and a very distinct population of females.

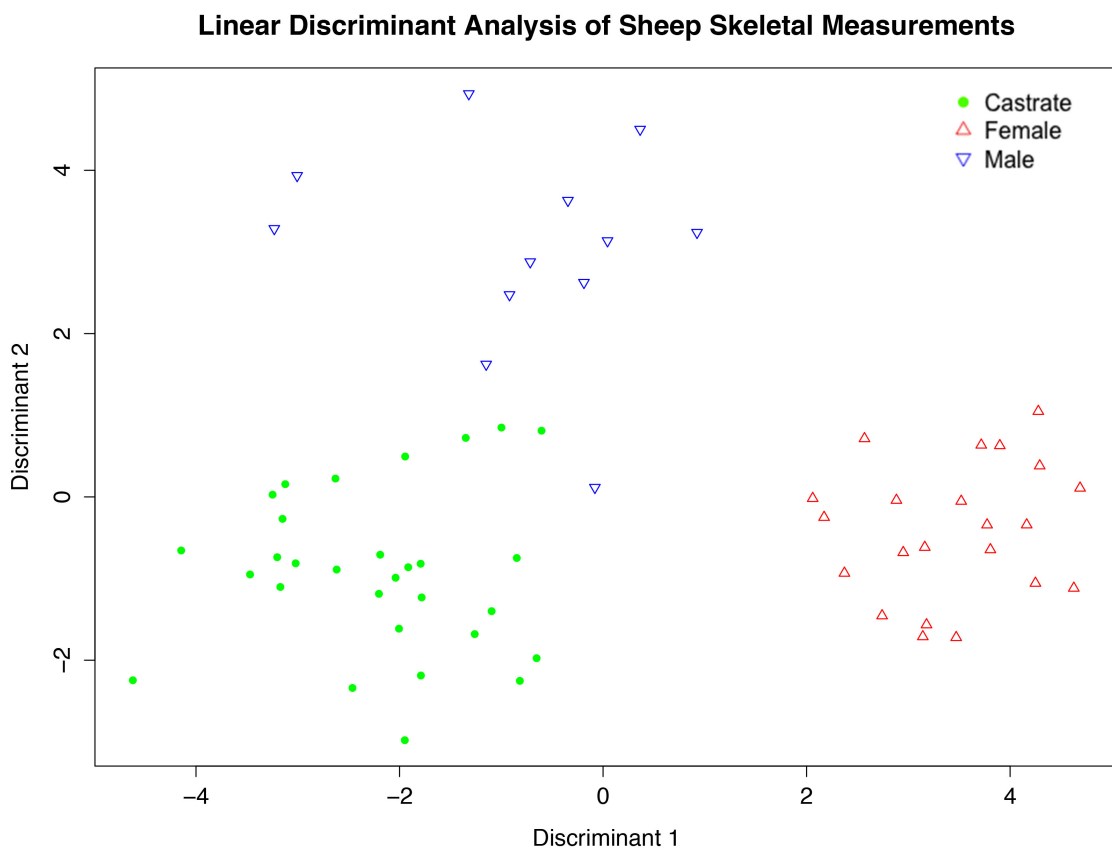


Figure 6.46: Plot displaying the linear discriminant function analysis of sheep long bone lengths, breadths, and circumferences, displaying the tight grouping of males, females, and castrates through the combination of all three factors. (Data from Davis, 2000, graph by author)

As the analysis of all the lengths and breadths gave such good results, an analysis was run on only the lengths and circumferences of all the major long bones. The statistical results were better than those for the lengths, breadths, and circumferences, with 75.72% of the variation accounted for by the first function ($df = 24$, $p < 0.0005$, Wilk's $\Lambda = 0.085$) and 24.28% by the second function ($df = 11$, $p < 0.0005$, Wilk's $\Lambda = 0.433$), but the graphical results are less distinct (**Figure 6.47**). It is clear from this graph that there is more overlap among the three groups, with castrates straying into both the male and female groups, but no overlap between the males and the females.

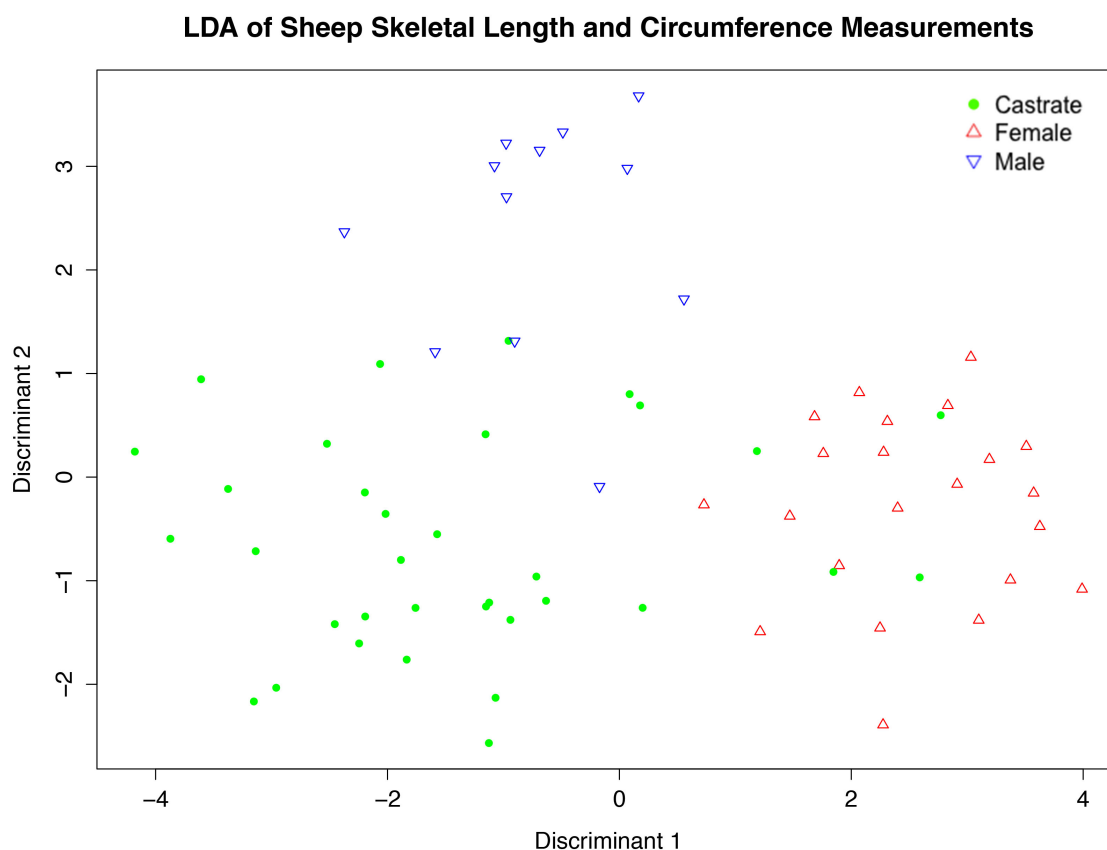


Figure 6.47: Graph showing results of the linear discriminant function analysis of the sheep long bone lengths and circumferences, displaying the linear relationship between males and females and overlap between castrates, females, and males. (Data from Davis, 2000, graph by author)

As the lengths and circumferences gave a good result, the lengths and breadths were also analysed to see what result they would give. They produced the best statistical result, with 78.55% of the variation in the variables accounted for by the first function ($df = 28$, $p < 0.0005$, Wilk's $\Lambda = 0.088$) and 21.45% of the variation accounted for by the

second function ($df = 13$, $p < 0.0005$, Wilk's $\Lambda = 0.463$). The graphical result is also superior to that of the analysis of the lengths and circumferences (**Figure 6.48**). There is a clear linear correlation between the males and females, with very little overlap, and most of the castrates are clustered away from both the males and the females, though a few castrates are intermixed with the males.

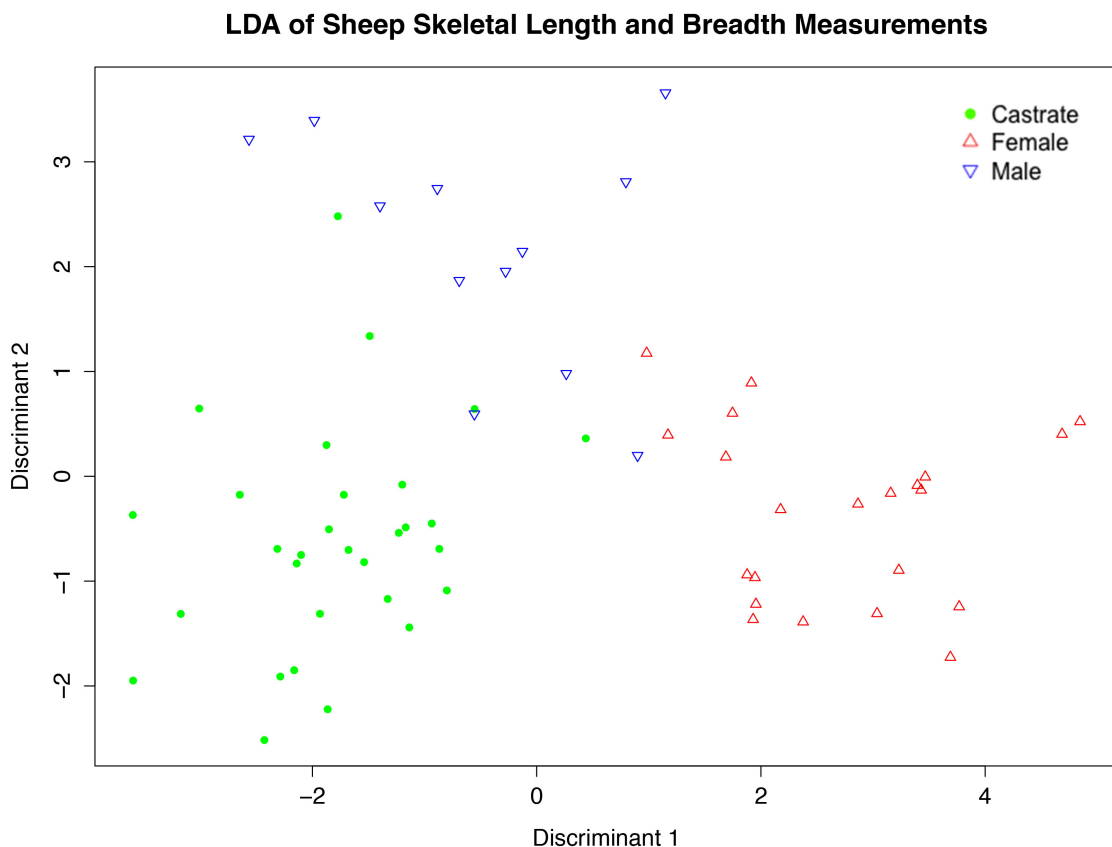


Figure 6.48: Graph showing the results of the linear discriminant function analysis of the sheep long bone lengths and breadths, displaying the very linear relationship between males and females, and slight overlap between castrates and males and males and females. (Data from Davis, 2000, graph by author)

In order to compare the results of the human osteological dataset, which could only use long bone lengths, an LDA of only the long bone lengths of the sheep was run. Statistically, the results for this analysis were the best of all of the sheep analyses, as the first function accounted for 87.22% of the variation within the series ($df = 12$, $p < 0.0005$, Wilk's $\Lambda = 0.242$), with the second function accounting for the remaining 12.78% ($df = 5$, $p < 0.0005$, Wilk's $\Lambda = 0.761$). However, as can be seen in **Figure 6.49**, the graphical representation of the analysis shows that the grouping is not as clear as that of the previous analyses. It is very similar to the graph of the human osteological LDA,

however, which may mean that, if long bone breadths could be added to the human osteological dataset, better discrimination of castrates might be achieved.

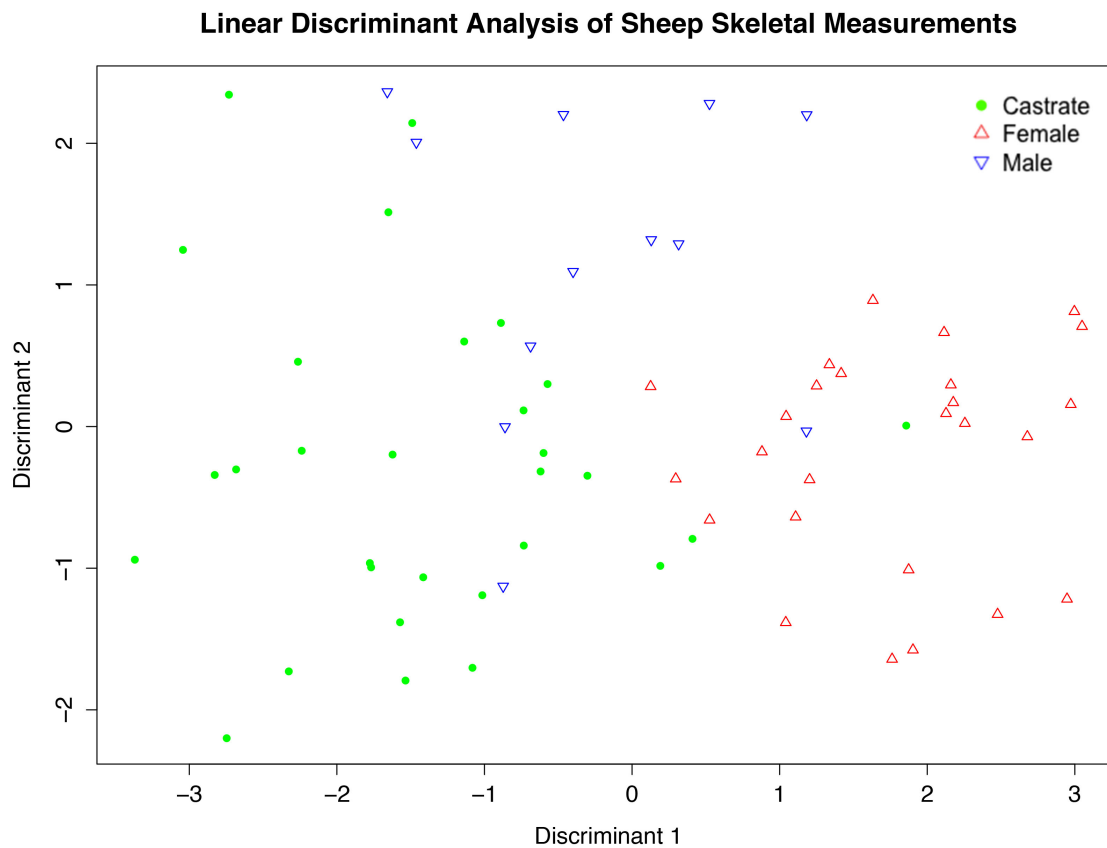


Figure 6.49: Graph showing the results of the linear discriminant function analysis of the sheep long bone lengths, displaying overlap among the castrates, males, and females. (Data from Davis, 2000, graph by author)

Overall, the linear discriminant function analysis of the sheep osteological data has shown that statistically, the lengths of the long bones of the skeleton give the best results, but that the lengths, epiphyseal breadths, and shaft circumferences of the long bones give the classification results, despite the lower proportion of trace in the first function. This may be because the shaft circumferences pull the males and females apart, while the epiphyseal breadths pull the castrates away from both the males and females.

The results shown with the sheep data demonstrate the excellent results that linear discriminant function analysis can give if a large and sufficiently robust dataset is available. The number of variables involved in the analysis of the sheep allowed for the easy and clear separation of the castrates from the males and females (with a few exceptions) and displayed the sort of linear relationship between the males and females that one would expect. More and better access to human skeletal population data

worldwide and more castrate skeletal data or the ability to transform more anthropometric data would allow for better and more accurate osteological analyses of human skeletal data, perhaps providing results as good as those of the human anthropometric and sheep osteometric datasets discussed here.